

NASA Technical Memorandum 89137

ANALYSIS OF ON-ORBIT THERMAL CHARACTERISTICS OF THE 15-METER HOOP/COLUMN ANTENNA

(NASA-TM-89137) ANALYSIS OF ON-ORBIT
THERMAL CHARACTERISTICS OF THE 15-METER
HOOP/COLUMN ANTENNA (NASA) 33 p CACL 22B

N87-21021

Unclas
G3/18 43593

Gregory C. Andersen
Jeffery T. Farmer
James Garrison

March 1987



National Aeronautics and
Space Administration

Langley Research Center
Hampton, Virginia 23665

ANALYSIS OF ON-ORBIT THERMAL CHARACTERISTICS OF THE 15-METER HOOP/COLUMN ANTENNA

Gregory C. Andersen and Jeffery T. Farmer
NASA Langley Research Center
Hampton, Virginia 23665

and

James Garrison
Rensselaer Polytechnic Institute
Troy, New York 12180

Abstract

In recent years, interest in large deployable space antennae has led to the development of the 15-meter hoop/column antenna. This scaled down version of a proposed operational antenna concept can be used for both ground and on-orbit testing. This paper examines the thermal environment the antenna is expected to experience during orbit and determines the temperature distributions leading to reflector surface distortion errors. Two flight orientations corresponding to 1) normal operation and 2) use in a Shuttle-attached flight experiment are examined. A reduced element model was used to determine element temperatures at 16 orbit points for both flight orientations. The temperatures ranged from a minimum of 188 K to a maximum of 326 K. Based on the element temperatures, orbit positions leading to possible worst case surface distortions were determined, and the subsequent temperatures were used in a static finite-element analysis to quantify surface control cord deflections. The predicted changes in the control cord lengths were in the sub-millimeter ranges; however, the sensitivity of the reflective surface to control cord length changes can result in large surface distortion errors.

Introduction

Over the past decade, interest in large space structures has increased dramatically. One category of large space structures that has been under study and development in the recent past is large, space-based, deployable antennae. Possible missions for such antenna concepts have ranged from mobile communication missions to Earth observation missions with antenna diameters ranging in size from 20 to 200 meters [1]. The large dimensions of the proposed antenna concepts have created difficulties in pre-flight verification because of the inability to adequately test the complete structure on the ground. To this end, development and construction of a viable antenna concept which could be used for both ground and flight test articles was initiated in the early 1980's [2]. One result of this program was a 15-meter-diameter hoop/column antenna. This antenna is a scaled down version of a 120-meter quad-aperture system proposed for use in the Land Mobile Satellite System (LMSS) [3] mission.

The 15-meter hoop/column antenna will allow adequate ground testing and on-orbit verification and still provide the structural and operational characteristics (i.e., structures, structural dynamics, radio frequency (RF) performance, deployment, etc.) that are inherent in the proposed large antenna concepts. Upon completion of ground testing, the antenna has been proposed to be upgraded for use in one of the flights of the Control of Flexible Structures (COFS) experiments which will utilize the Shuttle as a test bed for dynamic and flexible body control experiments [4]. The antenna also has possible application as a working microwave radiometer antenna after termination of the experimental testing.

The majority of past research and testing has focused on the structural aspects of the antenna: static and dynamic testing, static surface mesh management, etc. The study described in this paper examines the on-orbit temperatures that the antenna is expected to encounter, which can then be used as a focal point for possible upcoming thermal testing in a thermal vacuum facility and/or used in estimating the surface distortion that could occur on-orbit. The results presented in this study are derived from a first-order thermal analysis of the antenna based on possible operational and/or experimental environments and also include possible worst case conditions, by means of control cord deflections, for static reflector surface distortions.

Antenna Concept

The 15-meter hoop/column antenna is a tension-stabilized, centered, quad-aperture system with an effective focal length over diameter ratio of 0.62. (See Fig. 1.) It is composed of a triangular truss column fabricated of graphite/epoxy material and 48 hollow graphite/epoxy tubes which, when joined together with aluminum end fittings, form the outer hoop of the antenna. The tension elements underneath the reflecting surface are graphite cables and are used for management of the reflecting surface (through the use of the 96 control cables attached to the bottom of the column and the control surface). The cables connecting the hoop to the feed are fabricated of quartz material to provide minimal interference with the RF performance of the antenna. The reflecting surface of the antenna is gold-plated molybdenum wire mesh. The original hoop/column antenna was designed to operate in the 50- to 100-GHz frequency regions, which result in fairly stringent RF distortion requirements [root mean square (RMS) surface roughness on the order of 3 μ m]. This paper addresses one potential contribution to significant distortion errors, that of thermal distortion on-orbit.

Thermal Analysis

Thermal Analysis Program

To determine the temperature distributions that the antenna will be expected to encounter on-orbit, the Thermal Analyzer (TA) Program module in the Interactive Design and Evaluation of Advanced Spacecraft (IDEAS) program [5] is used. (For a more detailed discussion of program capabilities and

limitations, see Garrett [6].) This program will predict the temperature of each element of a finite-element model of a structure in Earth orbit. Technical capabilities for the TA program were developed by G. A. Howell of the General Dynamics Corporation, Convair Division, from the original work of Ballinger and Christensen [7]. Heat sources are solar radiation, Earth albedo, and Earth thermal radiation. The transient thermal response of each member is determined from an integration of energy absorbed from the three heat sources and reradiation of energy from the member to deep space. The position of the members relative to the Sun and the Earth is varied at 36 intervals in the orbit. Effects of Earth shadowing are also included. The analysis assures no radiation exchange or conduction between members and no shadowing of members by other members. Inputs to the thermal analyzer include the thermal properties of the structural members, the finite-element geometry and mass per unit area information, and orbital and orientation data for Sun/Earth/spacecraft geometry computations.

Thermal Model

The analytical model used for the thermal analysis in this report is not the full-order finite-element model that was used for the dynamic analysis performed on the antenna [8] because of element number limitations. (The full-order model contained over 7400 elements.) The reduced-order model was composed of 756 elements and accounts for only the major elements of the structure. (A less detailed model of the control surface tie system is used.) Figure 2 illustrates the reduced-order model. The use of the reduced model will not affect an accurate determination of the element temperatures because each element temperature is determined independently of the other elements. Therefore, although some of the less essential elements are eliminated, the temperatures of the major structural elements (such as the 96 surface control cable elements) are not different from those obtained using the full-order model.

The properties (both physical and material) were obtained from Ref. 9 and David Butler of NASA Langley Research Center. A summary of the thermal properties is shown in Table 1. The major thermal characteristics that are required by the Thermal Analyzer program are the material specific heat, emissivity, and solar absorptance. Because the analysis does not include conductivity calculations, those properties are not presented.

Thermal Cases

To determine the element temperature distributions that the hoop/column antenna could experience during normal operation or as part of the testing to be done in the COFS program, two different analysis cases were performed. The cases deal with two Earth-oriented flight paths which are as follows: (1) Earth oriented, nadir-pointing (normal mission operation orientation), and (2) Earth-oriented, pointing in the direction of the flight path (COFS configuration). The cases incorporated Shuttle-compatible orbital parameters (orbit altitude of 463 km and 28.5 degree inclination), and only the spacecraft orientation in the orbit was varied. For the two Earth oriented cases, element temperatures were calculated at 16 different points in the orbit.

Thermal Analysis Results

To aid in the explanation of the thermal results for each case analyzed, the discussion of temperatures will be limited to only two quadrants of the antenna. The first quadrant, quadrant X (see Fig. 3), has its centerline in the direction of the geometrical x-axis, and the second quadrant, quadrant Y, is in the direction of the y-axis. The antenna rays in the quadrants are numbered as shown in the figure. The elements that are of interest in each ray are the four graphite surface control cords (cords 1-4), the graphite hoop support cable, and the two quartz hoop support cables. The other elements of major interest are the hoop, column, and ray surface elements. These elements are shown in Figure 4. Figure 5 illustrates the two flight orientations with respect to the Earth. For the two orientations, temperature variations for the elements over the orbit were determined and plotted, and these graphs are presented in the Appendix. Selected results will be presented here and discussed in detail. Similar information can be obtained from the additional data presented in the Appendix. The results presented are in terms of the orbit position angle of the spacecraft as it flies through its prescribed orbit to identify the antenna's orientation relative to the Earth and Sun. At the initial orbit position of zero degrees and at a zero degree ascending node, the antenna is located directly between the Earth and Sun.

In general, it is expected that maximum differences in temperatures between the elements lead to maximum surface distortions or RMS surface error. Also, from previous research involving shape estimation of the reflective surface [10] it was found that the RMS surface error was more sensitive to changes in length of the outer control cords than the inner ones. In particular, control cord 3 had the greatest effect on RMS surface distortion and was used as the focal point for determining the thermal environment leading to possible worst case distortions. Because of the negative coefficient of thermal expansion, the control cords contract at temperatures higher than the 290 K reference temperature and expand at temperatures below 290 K. Consequently, maximum distortions are expected to occur when the majority of the tension cords are at the highest or at the lowest temperature. The lowest temperatures occur when the antenna is in the shadow. A determination of where the maximum temperatures (i.e., contractions) occur is not as straightforward, so a number of analyses were run as described below to establish this boundary.

Nadir Orientation

For one of the orientations examined, the spacecraft will fly in a nadir-pointing orientation (z-axis pointing toward the Earth's center) quadrant X is directed in the flight path, and quadrant Y is perpendicular to the orbit plane (POP). The combined orientation of the antenna in its orbit and the orientation of the structural elements in the antenna will result in different temperature profiles for each element. The elements of primary concern for figure distortion of the reflective surface are the four control cords, the graphite hoop support cord, the quartz hoop support cords, the hoop, and the column.

Figures 6 and 7 represent the temperature variations of the aforementioned cable elements for rays 4 and 10 (see Figure 3), as well as the hoop and column elements. From the results of the study, controller cable 4

and the graphite hoop support cable exhibited essentially the same temperature variation; therefore, only the temperature variation for controller cable 4 is presented. The element temperatures ranged from 189 to 326 K. An examination of the temperature fluctuations shows that the controller cord elements in ray 4 will reach a peak temperature near the 337.5 degree orbit point, whereas the quartz element reaches a peak near 22.5 degrees. This is due to the orientation of the elements relative to the incoming solar flux. (Earth thermal heating and albedo heating are not determining factors because the elements are at a constant orientation relative to the Earth for the nadir flight orientation.) At these points, the controller cords are nearly perpendicular to the incoming flux which results in the higher temperatures. An examination of the temperature variations for the elements in ray 10 shows that the outer graphite cord elements (cords 3 and 4) reach their maximum temperature near the zero degree orbit angle. During the time these outer elements are in view of the Sun, slight variation in the temperature is detected because the orientation of ray 10 to the Sun leads to reduced changes in the orientation of the elements with respect to the incoming solar flux. The inner cords, however, do exhibit temperature fluctuations because of the differing orientations from those of the outer cords. The decrease in element temperatures during a part of the time the antenna is in the Sun is due to the elements becoming parallel to the solar flux, which reduces the amount of area of each element exposed to the Sun.

The major decrease in temperatures for both rays occurs from entry into the Earth's shadow at an orbit position of 112.5 degrees. Exit from the shadow occurs at 247.5 degrees. As the antenna proceeds through the shadow, the elements cool down to a minimum temperature level in the 190 K range. The structural elements do not, however, reach an equilibrium temperature, which would be evident by a constant temperature over a range of orbit angles. Upon exiting the shadow, the elements heat rapidly because their relatively low thermal inertia allows rapid changes in temperature.

To determine the orbit position where large surface distortions may occur from contraction of the control cords, the largest temperature difference (occurring above the reference temperature) between the control cords and the other hoop, column, and quartz elements must be found. This can be seen from the temperature plots to occur at approximately the 337.5 degree orbit angle. As was stated earlier, the largest surface distortions due to element elongation will occur at the coldest point in the shadow (or an orbit angle of 247.5 degrees). From the temperature profiles for these two cases, a static analysis of the simplified finite-element model of the hoop/column was performed for estimations of the deflections of the elements, and the results are presented later.

Flight Path Orientation

The other flight orientation of the antenna examined consisted of a negative 90 degree rotation from the nadir orientation about the POP axis which results in the column being aligned along the negative direction of the flight path and the centerline of the X quadrant pointing in the nadir direction. Temperature plots for the same elements that were used in the nadir orientation discussion are shown in Figures 8 and 9. For this orientation, the element temperatures ranged from 188 to 326 K. The temperature range did not vary significantly from that found in the nadir orientation. The major difference is in the temperature variations between elements at the same orbit points. The variations, again, are due entirely to the orientation of the elements to the incoming heat flux from the various sources of heat. The controller cables in ray 4 reach maximum temperatures for orbit angles ranging from 22.5 to 67.5 degrees with the quartz element temperatures at a local minimum. As was the case for the nadir orientation, the elements reach minimum temperatures when in the shadow.

The orbit points which will lead to possible worst case surface distortions for this flight orientation are at a 45 degree orbit angle (for maximum contraction) and at the coldest part of the shadow period (for maximum elongation). The maximum contraction of the control cables will occur at 45 degrees because the control elements are near their maximum temperatures (control cord 3 has its maximum at 45 degrees), while the quartz elements are at a local minimum at this orbit angle and the hoop and column elements are decreasing in temperature. All these factors combined should lead to the maximum contraction of the control cables (in particular control cable 3). Again, a static analysis of the finite-element model using these temperature profiles was performed for estimations on deflection lengths of the elements.

Static Analyses

A number of finite-element static analyses were performed using the previously determined element temperatures to estimate control cord length changes which will result in reflective surface distortions. Two static analyses were performed for each flight orientation: the first corresponds to the orbit point where the predicted maximum contraction of the control cords will occur, and the second is the point in the orbit where predicted maximum elongation will occur. Because the finite-element model used in the analysis was a reduced-order model, an accurate estimate of the surface distortions is not possible. Therefore, for this analysis, attention was paid primarily to the effects of on-orbit temperatures on the changes in length of the surface control cords. These length changes can then, in turn, be used later in a surface contour program [11] to determine estimated surface distortions.

The results of the four static analyses (two cases for each orientation) are shown in Tables 2, 3, 4, and 5. Distortions of the control cords in all 24 rays of the antenna are presented for a better understanding of overall distortions and for direct use in the aforementioned surface estimation program. The first two figures correspond to the nadir orientation. The maximum changes in length occur at minimum rather than maximum control cord temperatures because of the larger deviation from the reference temperature. The elongations of control cord 3 reached a maximum of 0.326 mm, and the contractions reached a maximum of -0.0721 mm. Therefore, the thermal loads resulted in sub-millimeter changes in cord length. The results are very similar for the flight path orientation. The largest changes in length occurred when the control cords were at their coldest temperature. The maximum elongation of control cord 3 was 0.326 mm, and the maximum contraction was -0.082 mm. The maximum elongation and contraction did not vary significantly from those of the nadir orientation. At first glance, the results would seem to indicate that the thermal effects do not seem significant because the length changes are small. However, based on preliminary estimates of the effects on surface distortions [11], these slight changes in cord length can be magnified in the surface distortion errors. (At some points on the antenna, the 0.326-mm change in cord length can result in surface distortions as high as 1.3 mm--a 4 to 1 magnification.) Because of the antenna surface sensitivity to changes in control cord length and the reflective surface shape accuracy that is required for this concept, further static analyses of the surface distortions are recommended.

Conclusion

A thermal analysis of the 15-meter hoop/column antenna was performed. The expected on-orbit temperatures were determined at various points throughout the orbit for two attitude orientations corresponding to a normal flight operation orientation and the proposed Control of Flexible Structures program orientation. The element temperatures ranged from a minimum of 188 K, occurring when the antenna is in the Earth's shadow, to a maximum of 326 K. The element temperatures were then used in a finite-element analysis to determine static distortions due to the thermal environment. For each orientation, two static analysis cases were performed, using the element temperatures corresponding to the two orbit positions where possible worst case surface distortions will occur. The first is due to contraction of the surface control cords, and the second, to elongation of the control cords. The resulting changes in length of the control cords were in the sub-millimeter region. However, because of the sensitivity of the reflective surface to changes in the length of the control cords, these small length changes can manifest themselves in large surface root mean square errors. Further, more detailed static analyses are required to obtain a better understanding of the complete thermal environment effects on the antenna and its performance.

References

1. Lovelace, U. M. and Garrett, L. B.: "Large Space Systems Requirements, Deployable Concepts, and Technology Issues," Presented at the AAS 33rd Annual Meeting, Boulder, CO, AAS 86-394, October 26-29, 1986.
2. Sullivan, M. R.: "LSST (Hoop/Column) Maypole Antenna Development Program," NASA CR-3558, Part 2, Harris Corporation, Contract NAS1-15763, June 1982.
3. Golden, C. T.; Lackey, J. A.; and Spear, E.: "Configuration Development of the Land Mobile Satellite System (LMSS) Spacecraft," Large Space Systems Technology, 1981, Williams J. Boyer, compiler, NASA CP-2215, Part 2, 1982, pp. 717-760.
4. Pyle, J. S. and Montgomery, R.: "COFS II 3-D Dynamics and Controls Technology," NASA/DOD Control/Structures Interaction Technology, NASA CP-2447, Part 1, November 1986, pp. 327-345.
5. Leondis, Alex: "Large Advanced Space Systems Computer-Aided Design and Analysis Program," NASA CR-159191-1, General Dynamics Convair Division, Contract NAS1-15462, July 1980.
6. Garrett, L. B.: "Thermal Modeling and Analysis of Structurally Complex Spacecraft Using the IDEAS System," AIAA Paper No. 83-1459, 1983.
7. Ballinger, J. C. and Christensen, E. H.: "Environmental Control Study of Space Vehicles. (Part II), Thermal Environment of Space - Supplement A: Graphical Presentation of Solar, Planetary Thermal and Planetary Albedo Radiation Incident to Space Vehicles," ERR-AN-016, Eng. Dept., General Dynamics/Convair Division, January 1961.
8. Belvin, W. K. and Edighoffer, H. H.: "15 Meter Hoop-Column Antenna Dynamics: Test and Analysis," NASA/DOD Control/Structures Interaction Technology, NASA CP-2447, Part 1, November 1986, pp. 167-185.
9. Harris Corporation: "Development of the 15-Meter Diameter Hoop Column Antenna-- A Final Report," NASA CR-4038, December 1986.
10. Belvin, W. K.; Edighoffer, H. H.; and Herstrom, C. L.: "Quasi-Static Shape Control of a 15 Meter Hoop Column Antenna," To be Presented at the AIAA/ASME/ASCE/AHS 28th Structures, Structural Dynamics and Materials Conference, Monterey, California, April 6-8, 1987.

Table 1. Hoop/Column Thermal Properties.

ELEMENT	*CTE	ABSORPTION	EMITTANCE	**C _p
Teflon-Coated Quartz Cables	0.7 E-7	0.25	0.89	1.004
Teflon-Coated Graphite Cables	-5.0 E-7	0.90	0.90	0.857
Graphite/Epoxy Structural Components	-4.4 E-7	0.90	0.90	0.857

* CTE--Coefficient of Thermal Expansion, °C⁻¹

** C_p --Specific Heat, kJ/kg °K

Table 2. Control Cord Deflections Caused by Hot Point in Orbit in Nadir Orientation (+ elongation).

RAY	CORD 1 (mm)	CORD 2 (mm)	CORD 3 (mm)	CORD 4 (mm)
1	-1.137E-02	-3.942E-02	-6.044E-02	-1.248E-02
2	-1.439E-02	-4.195E-02	-6.228E-02	-1.528E-02
3	-1.598E-02	-4.310E-02	-6.220E-02	-1.506E-02
4	-1.227E-03	-2.054E-02	-7.207E-02	-8.857E-03
5	-1.598E-02	-4.310E-02	-6.225E-02	-1.506E-02
6	-1.439E-02	-4.195E-02	-6.228E-02	-1.528E-02
7	-1.137E-02	-3.942E-02	-6.044E-02	-1.248E-02
8	-7.371E-03	-3.521E-02	-5.724E-02	-8.298E-03
9	-1.588E-03	-2.851E-02	-5.045E-02	-2.565E-04
10	5.301E-03	-1.908E-02	-3.995E-02	1.204E-02
11	1.335E-02	-6.378E-03	-2.478E-02	2.893E-02
12	2.316E-02	1.002E-02	-4.935E-03	5.234E-02
13	3.394E-02	3.056E-02	2.119E-02	8.338E-02
14	4.395E-02	5.449E-02	5.232E-02	1.210E-01
15	5.194E-02	7.907E-02	8.592E-02	1.646E-01
16	5.561E-02	9.659E-02	1.110E-01	1.886E-01
17	5.194E-02	7.907E-02	8.592E-02	1.646E-01
18	4.395E-02	5.449E-02	5.232E-02	1.210E-01
19	3.394E-02	3.056E-02	2.119E-02	8.338E-02
20	2.316E-02	1.002E-02	-4.935E-03	5.234E-02
21	1.335E-02	-6.378E-03	-2.478E-02	2.893E-02
22	5.301E-03	-1.908E-02	-3.995E-02	1.204E-02
23	-1.588E-03	-2.851E-02	-5.045E-02	-2.565E-04
24	-7.371E-03	-3.521E-02	-5.724E-02	-8.298E-03

Table 3. Control Cord Deflection Caused by Cold Point in Orbit in Nadir Orientation (+ elongation).

RAY	CORD 1 (mm)	CORD 2 (mm)	CORD 3 (mm)	CORD 4 (mm)
1	2.220E-01	2.533E-01	3.221E-01	5.994E-01
2	2.216E-01	2.532E-01	3.219E-01	5.971E-01
3	2.221E-01	2.537E-01	3.231E-01	6.005E-01
4	2.512E-01	2.998E-01	3.044E-01	6.163E-01
5	2.221E-01	2.537E-01	3.231E-01	6.005E-01
6	2.216E-01	2.532E-01	3.219E-01	5.971E-01
7	2.220E-01	2.533E-01	3.221E-01	5.994E-01
8	2.218E-01	2.531E-01	3.213E-01	6.000E-01
9	2.221E-01	2.532E-01	3.215E-01	6.017E-01
10	2.249E-01	2.533E-01	3.218E-01	6.050E-01
11	2.225E-01	2.536E-01	3.222E-01	6.066E-01
12	2.223E-01	2.537E-01	3.225E-01	6.090E-01
13	2.227E-01	2.545E-01	3.239E-01	6.130E-01
14	2.227E-01	2.545E-01	3.239E-01	6.139E-01
15	2.229E-01	2.552E-01	3.252E-01	6.160E-01
16	2.230E-01	2.554E-01	3.256E-01	6.176E-01
17	2.229E-01	2.552E-01	3.252E-01	6.160E-01
18	2.227E-01	2.545E-01	3.239E-01	6.139E-01
19	2.227E-01	2.545E-01	3.239E-01	6.130E-01
20	2.223E-01	2.537E-01	3.225E-01	6.090E-01
21	2.225E-01	2.536E-01	3.222E-01	6.066E-01
22	2.249E-01	2.533E-01	3.218E-01	6.050E-01
23	2.221E-01	2.532E-01	3.215E-01	6.017E-01
24	2.218E-01	2.531E-01	3.213E-01	6.000E-01

Table 4. Control Cord Deflections Caused by Hot Point in Orbit in Flight Orientation (+ elongation).

RAY	CORD 1 (mm)	CORD 2 (mm)	CORD 3 (mm)	CORD 4 (mm)
1	-4.568E-02	-6.005E-02	-7.380E-02	-2.896E-02
2	-4.697E-02	-5.913E-02	-6.881E-02	-2.487E-02
3	-4.758E-02	-5.772E-02	-6.436E-02	-1.760E-02
4	-2.314E-02	-8.369E-03	-8.202E-02	-2.736E-03
5	-4.758E-02	-5.772E-02	-6.436E-02	-1.760E-02
6	-4.697E-02	-5.913E-02	-6.881E-02	-2.487E-02
7	-4.568E-02	-6.005E-02	-7.380E-02	-2.896E-02
8	-4.382E-02	-5.954E-02	-7.631E-02	-3.243E-02
9	-4.084E-02	-5.712E-02	-7.517E-02	-3.124E-02
10	-3.691E-02	-5.133E-02	-6.873E-02	-2.254E+01
11	-3.151E-02	-4.007E-02	-5.391E-02	-5.304E-03
12	-2.495E-02	-2.533E-02	-3.290E-02	2.107E-02
13	-1.845E-02	-7.653E-03	-4.488E-03	5.825E-02
14	-1.292E-02	1.199E-02	3.014E-02	1.044E-01
15	-8.631E-03	3.086E-02	6.795E-02	1.569E-01
16	-7.727E-03	4.002E-02	9.319E-02	1.844E-01
17	-8.631E-03	3.086E-02	6.795E-02	1.569E-01
18	-1.292E-02	1.199E-02	3.014E-02	1.044E-01
19	-1.845E-02	-7.653E-03	-4.488E-03	5.825E-02
20	-2.495E-02	-2.533E-02	-3.290E-02	2.107E-02
21	-3.151E-02	-4.007E-02	-5.391E-02	-5.304E-03
22	-3.691E-02	-5.133E-02	-6.873E-02	-2.254E+01
23	-4.084E-02	-5.712E-02	-7.517E-02	-3.124E-02
24	-4.382E-02	-5.954E-02	-7.631E-02	-3.243E-02

Table 5. Control Cord Deflections Caused by Cold Point in Orbit in Flight Orientation (+ elongation).

RAY	CORD 1 (mm)	CORD 2 (mm)	CORD 3 (mm)	CORD 4 (mm)
1	2.129E-01	2.473E-01	3.197E-01	6.029E-01
2	2.137E-01	2.493E-01	3.224E-01	6.041E-01
3	2.148E-01	2.510E-01	3.254E-01	6.103E-01
4	2.460E-01	3.016E-01	3.060E-01	6.281E-01
5	2.148E-01	2.510E-01	3.254E-01	6.103E-01
6	2.137E-01	2.493E-01	3.224E-01	6.041E-01
7	2.129E-01	2.473E-01	3.197E-01	6.029E-01
8	2.117E-01	2.443E-01	3.147E-01	5.988E-01
9	2.114E-01	2.423E-01	3.115E-01	5.963E-01
10	2.110E-01	2.413E-01	3.097E-01	5.974E-01
11	2.114E-01	2.423E-01	3.115E-01	6.005E-01
12	2.117E-01	2.442E-01	3.147E-01	6.067E-01
13	2.126E-01	2.469E-01	3.197E-01	6.149E-01
14	2.131E-01	2.487E-01	3.223E-01	6.191E-01
15	2.138E-01	2.504E-01	3.252E-01	6.233E-01
16	2.141E-01	2.511E-01	3.262E-01	6.256E-01
17	2.138E-01	2.504E-01	3.252E-01	6.233E-01
18	2.131E-01	2.487E-01	3.223E-01	6.191E-01
19	2.126E-01	2.469E-01	3.197E-01	6.149E-01
20	2.117E-01	2.442E-01	3.147E-01	6.067E-01
21	2.114E-01	2.423E-01	3.115E-01	6.005E-01
22	2.110E-01	2.413E-01	3.097E-01	5.974E-01
23	2.114E-01	2.423E-01	3.115E-01	5.963E-01
24	2.117E-01	2.443E-01	3.147E-01	5.988E-01

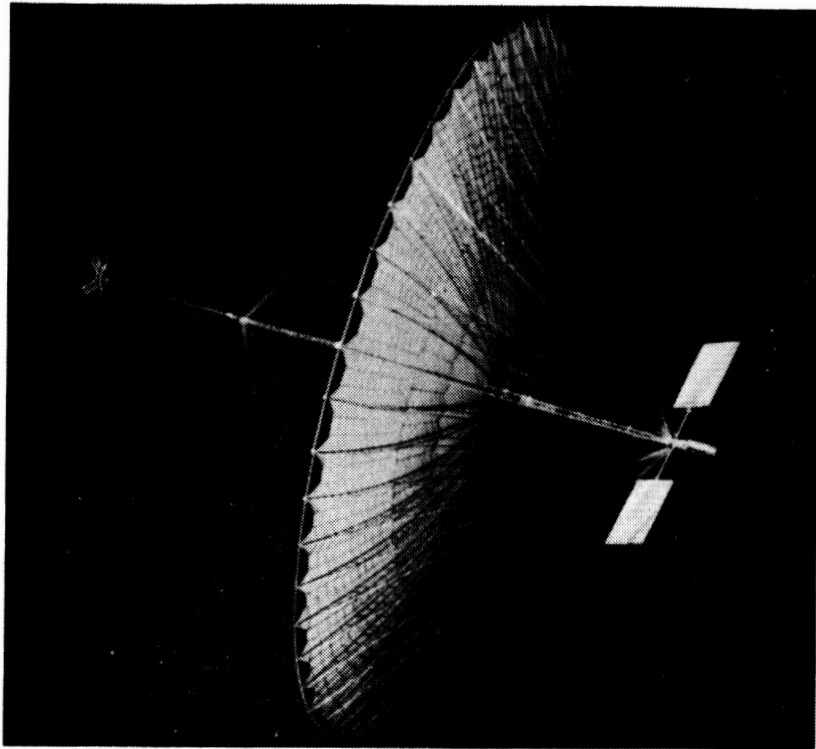
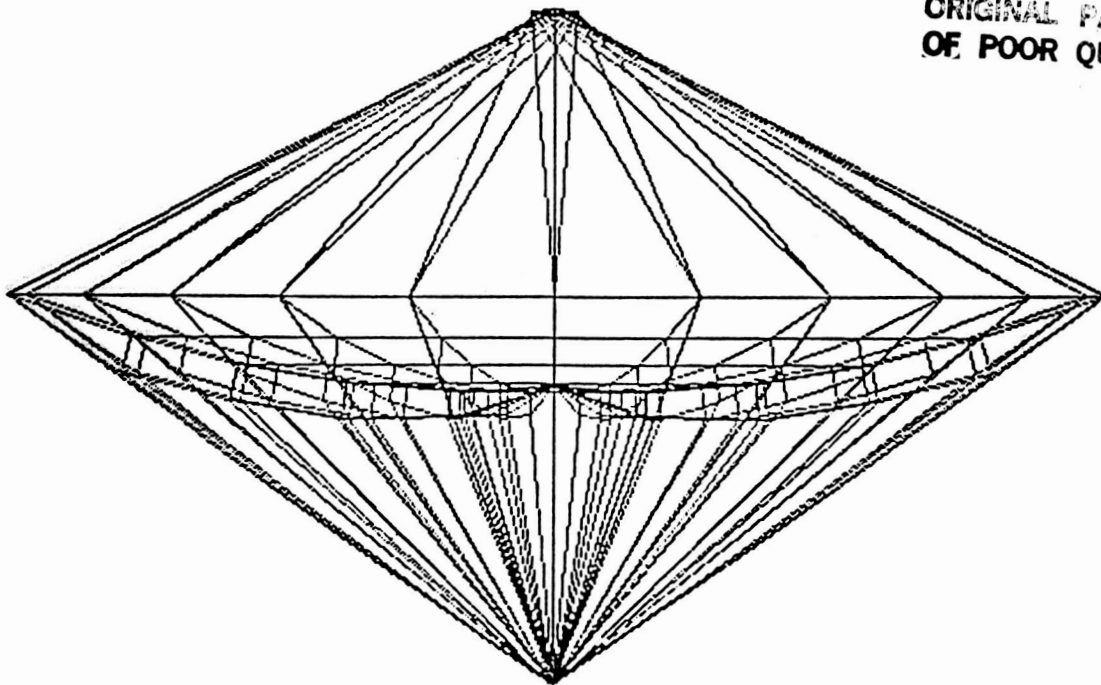


Figure 1. Hoop/Column Antenna.



ORIGINAL PAGE IS
OF POOR QUALITY

Figure 2. Reduced-Order Hoop/Column Model.

ORIGINAL PAGE IS
OF POOR QUALITY

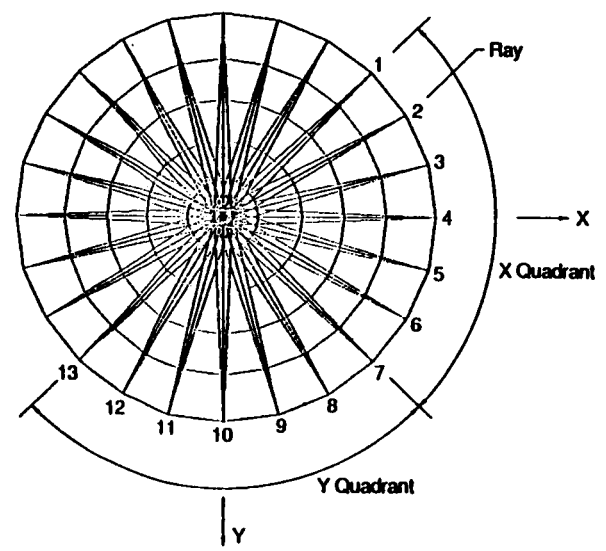


Figure 3. Hoop/Column Quadrants and Rays.

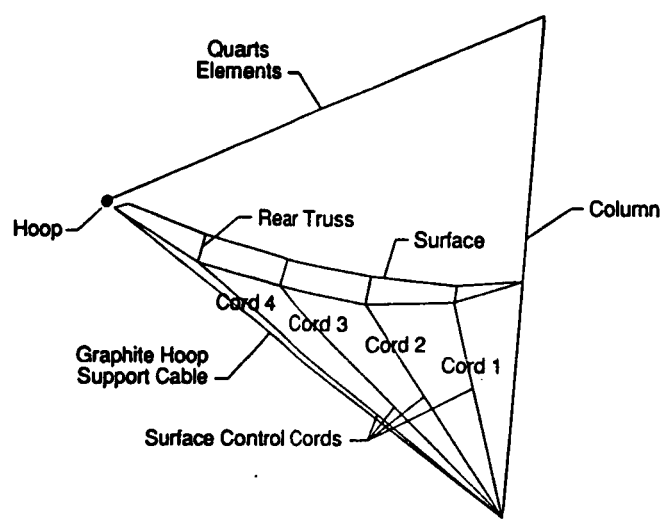


Figure 4. Hoop/Column Ray Elements.

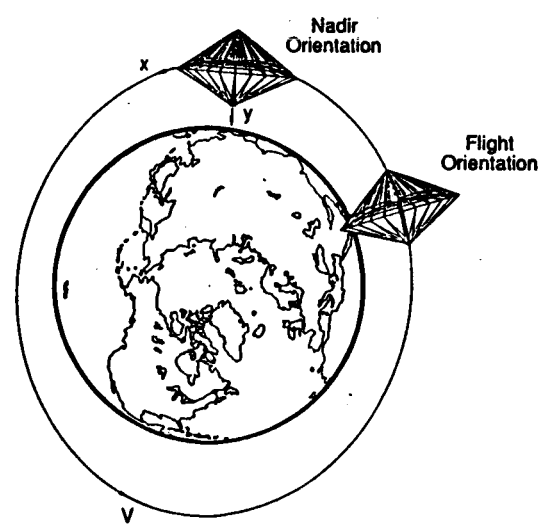


Figure 5. Flight Orientations Examined in Study.

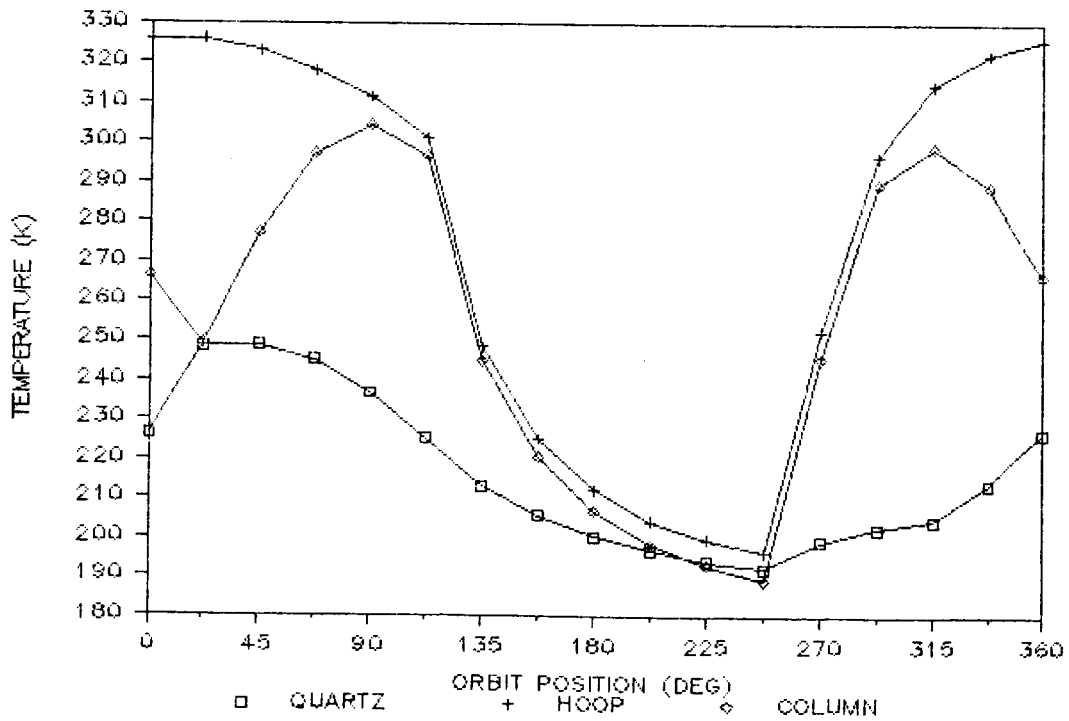
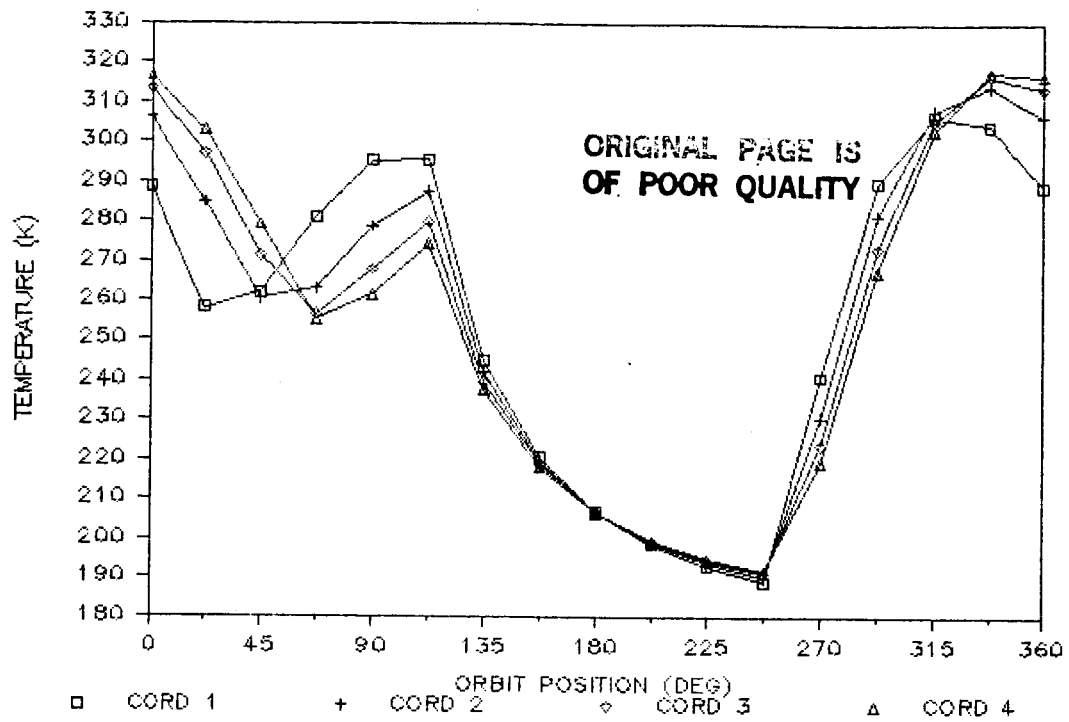


Figure 6. Element Temperature Variation for Ray 4 in Nadir Orientation.

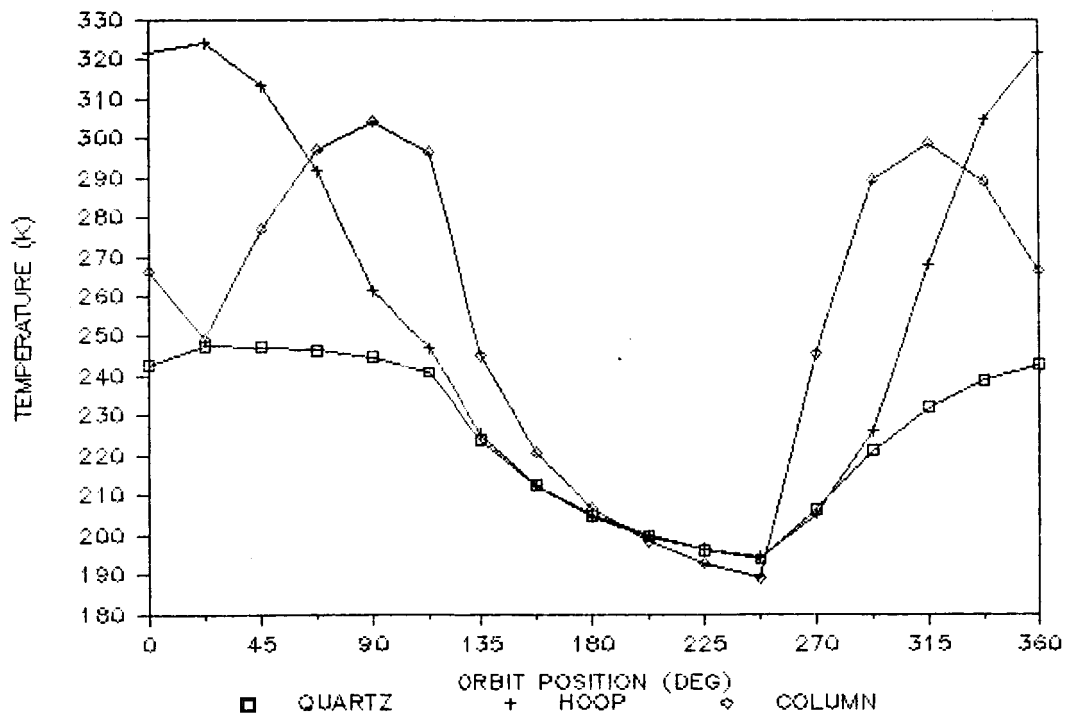
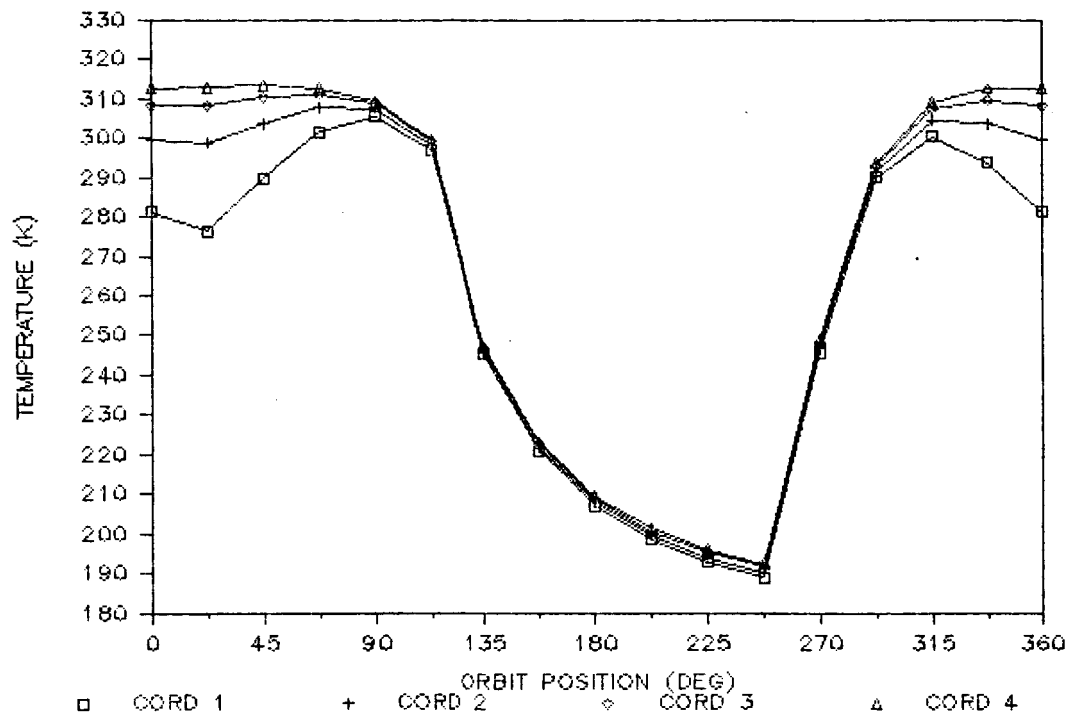


Figure 7. Element Temperature Variation for Ray 10 in Nadir Orientation.

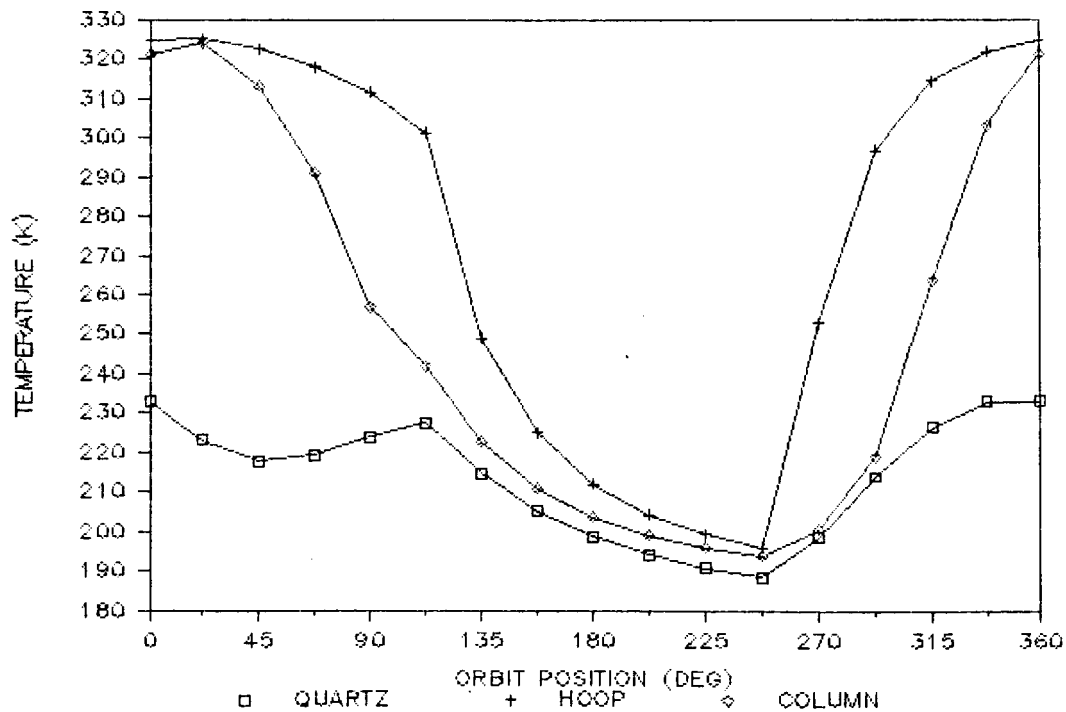
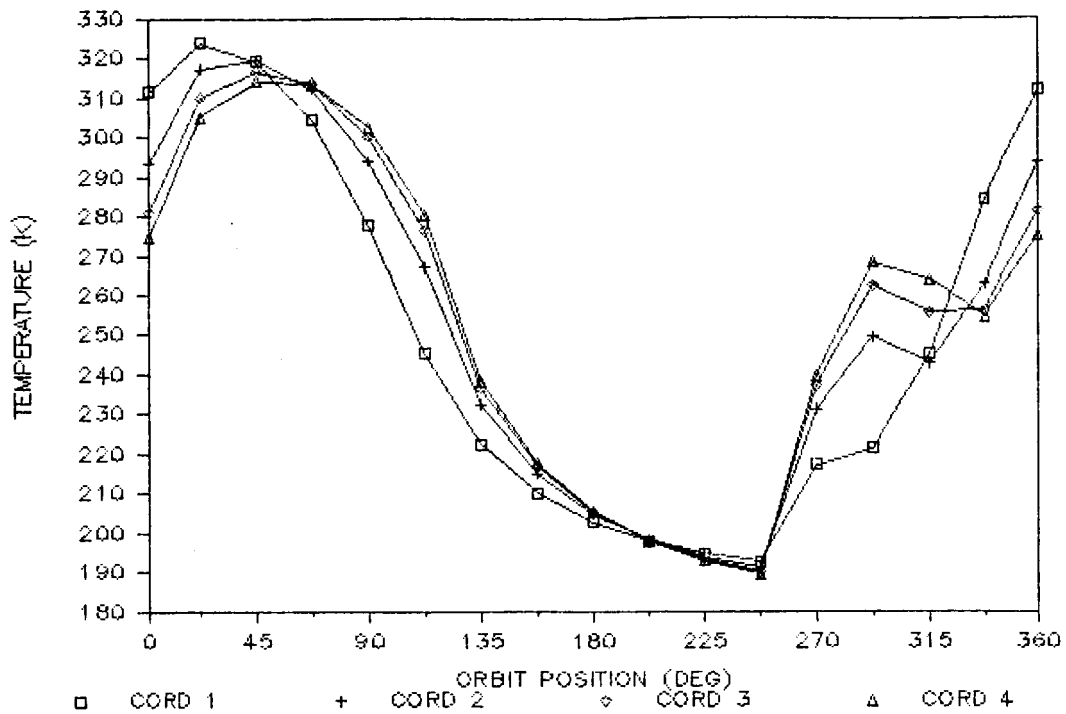


Figure 8. Element Temperature Variation for Ray 4 in Flight Orientation.

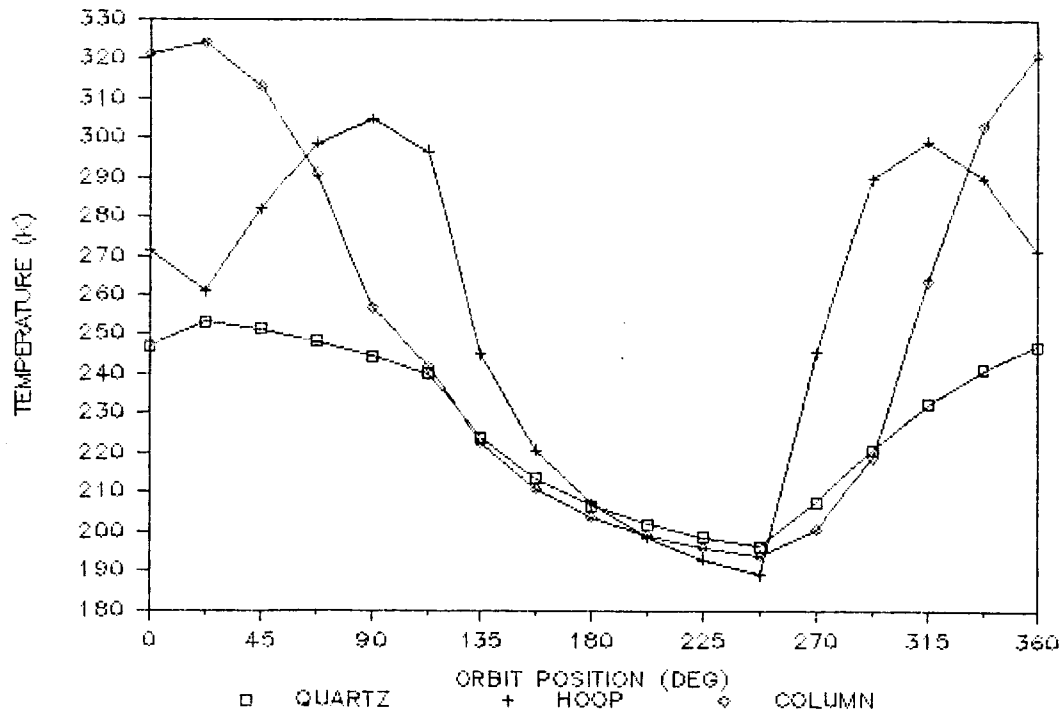
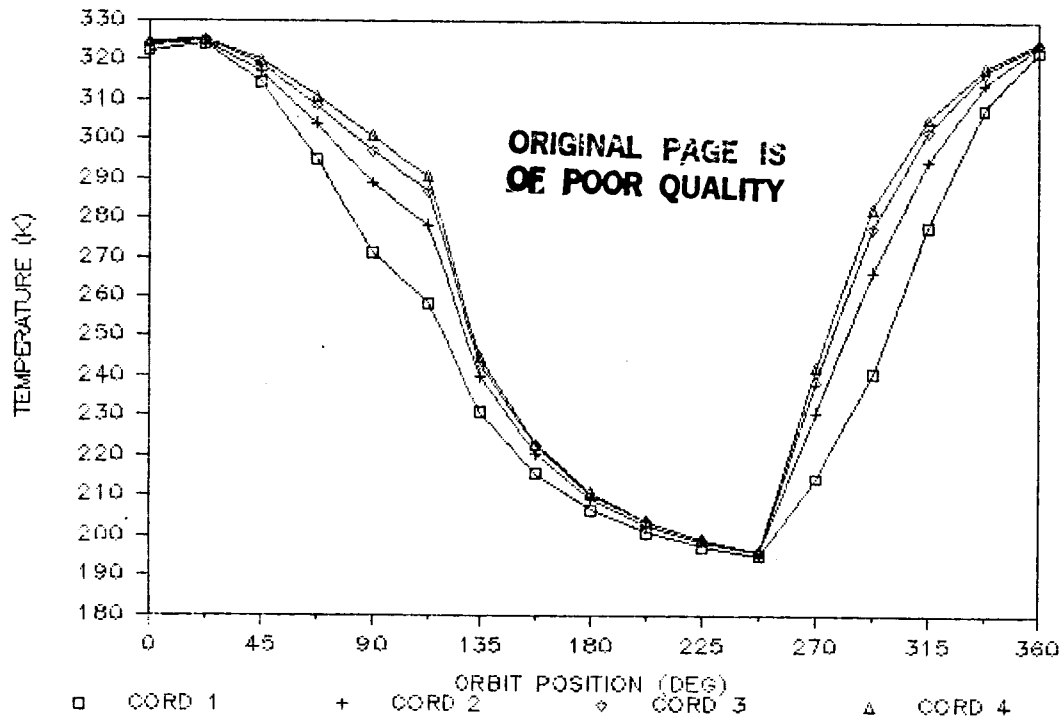
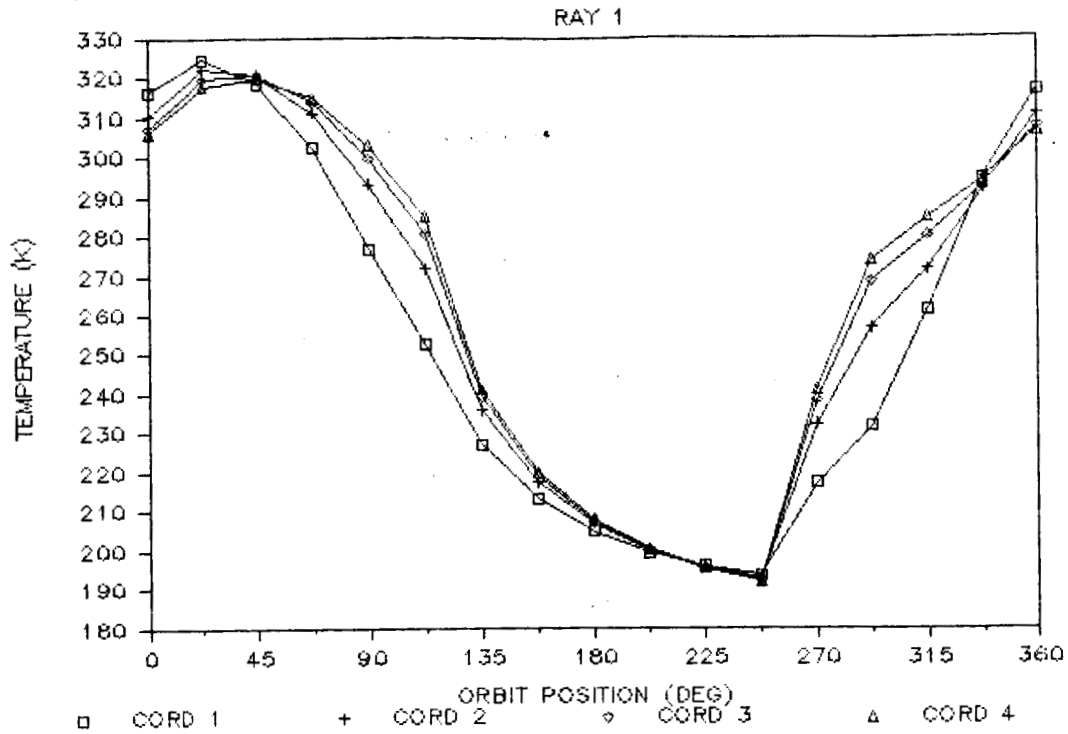


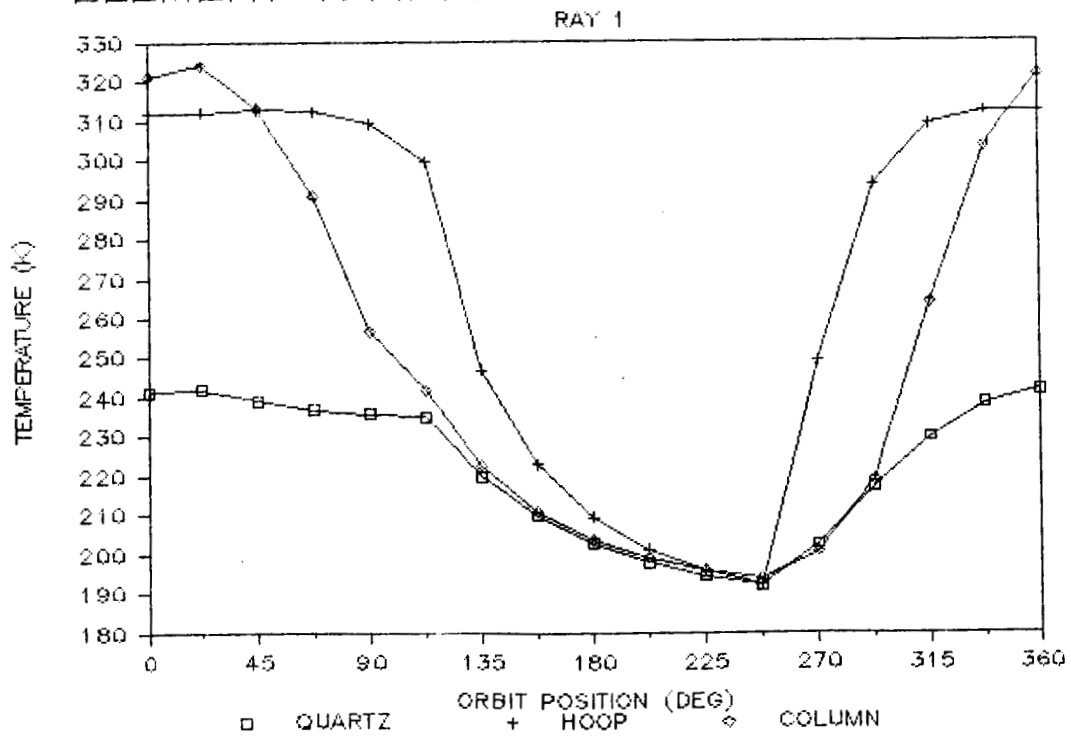
Figure 9. Element Temperature Variation for Ray 10 in Flight Orientation.

APPENDIX. ELEMENT TEMPERATURE VARIATIONS (CONT.)

ELEMENT TEMPERATURE VARIATION FLIGHT

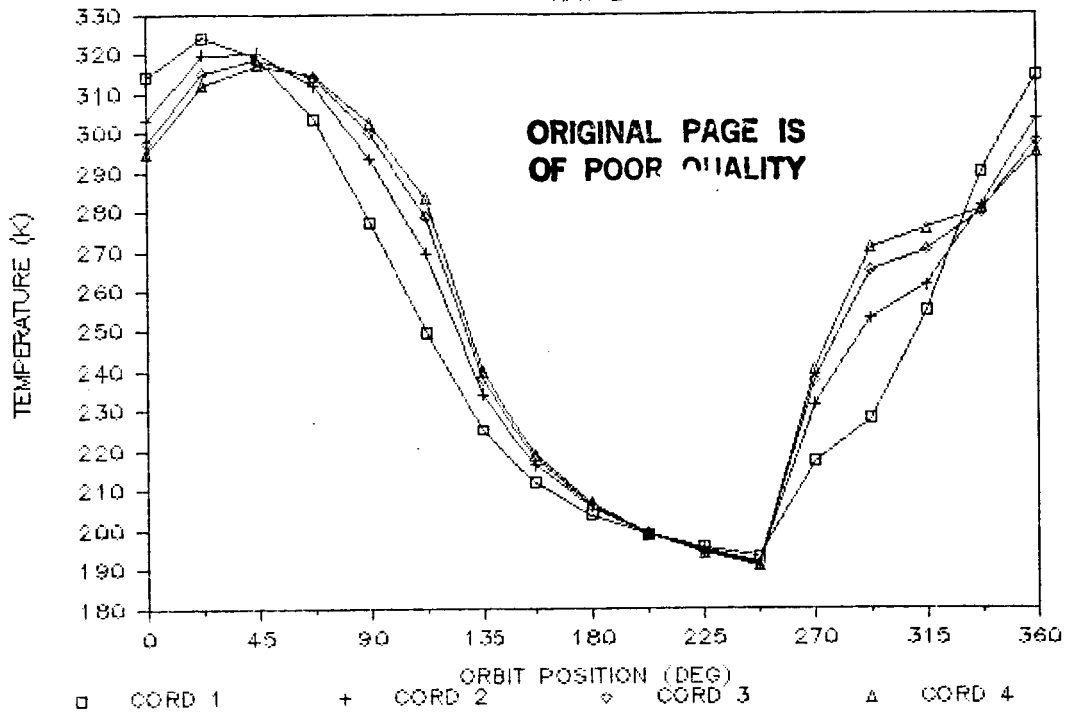


ELEMENT TEMPERATURE VARIATION FLIGHT

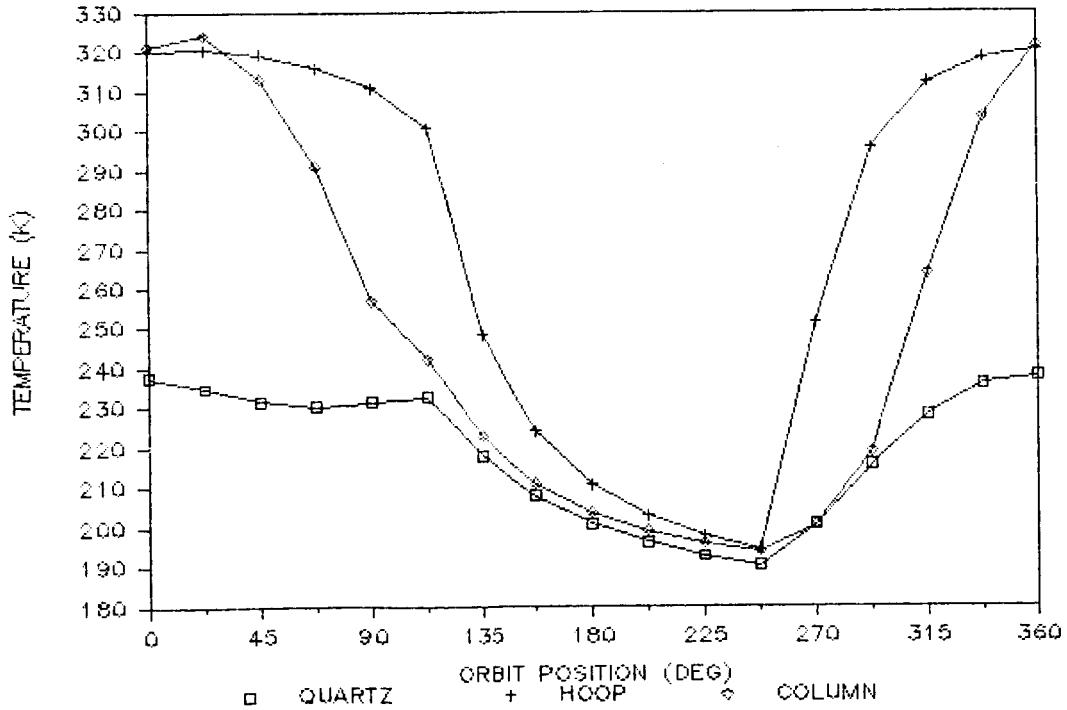


APPENDIX. ELEMENT TEMPERATURE VARIATIONS (CONT.)

ELEMENT TEMPERATURE VARIATION FLIGHT RAY 2



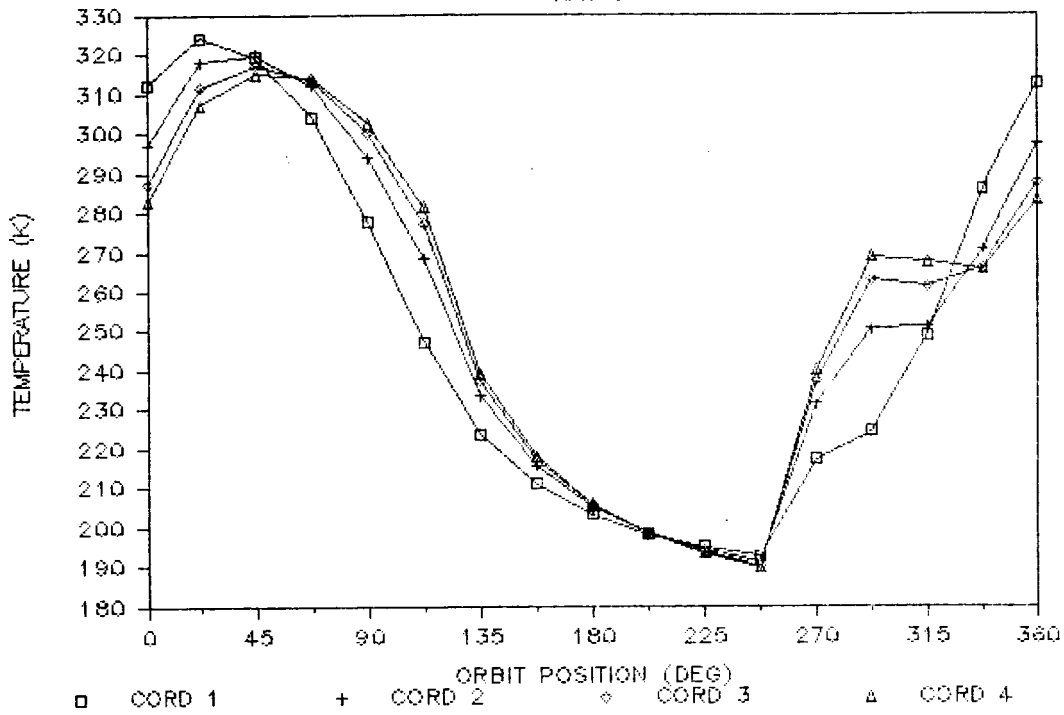
ELEMENT TEMPERATURE VARIATION FLIGHT RAY 2



APPENDIX. ELEMENT TEMPERATURE VARIATIONS (CONT.)

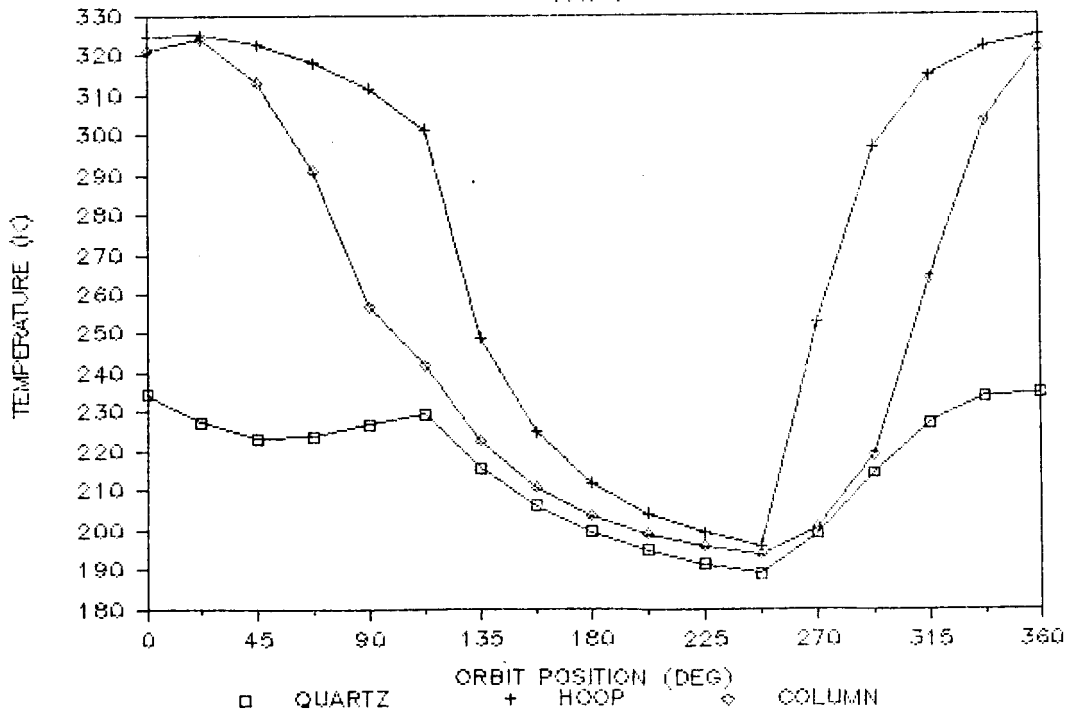
ELEMENT TEMPERATURE VARIATION FLIGHT

RAY 3



ELEMENT TEMPERATURE VARIATION FLIGHT

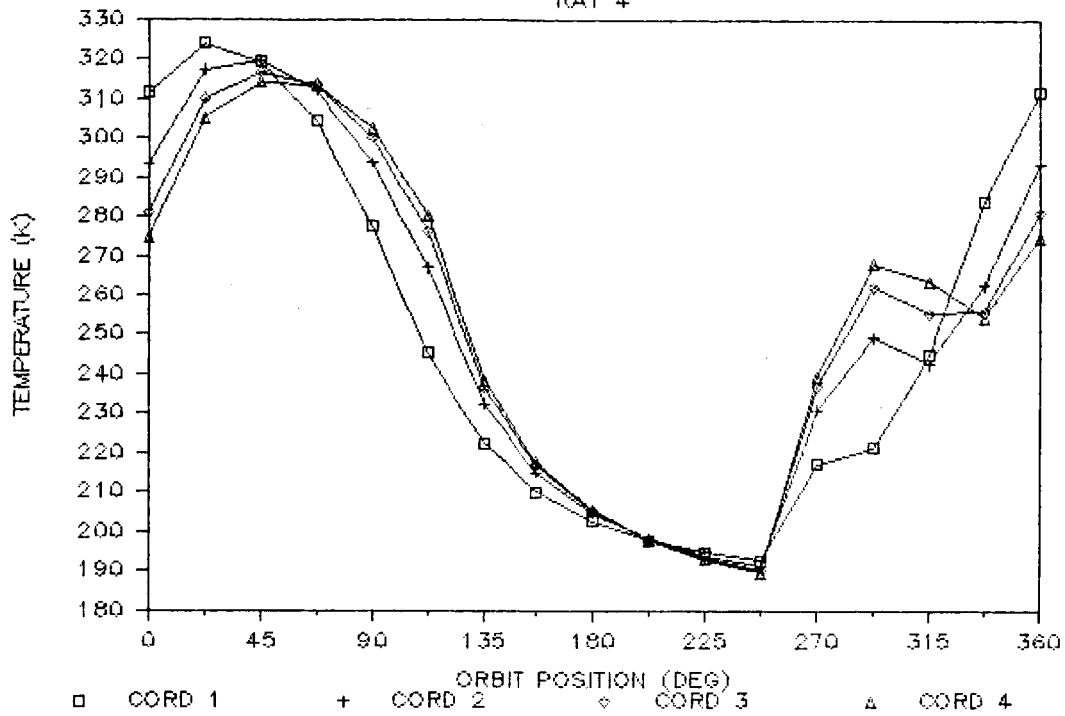
RAY 3



APPENDIX. ELEMENT TEMPERATURE VARIATIONS (CONT.)

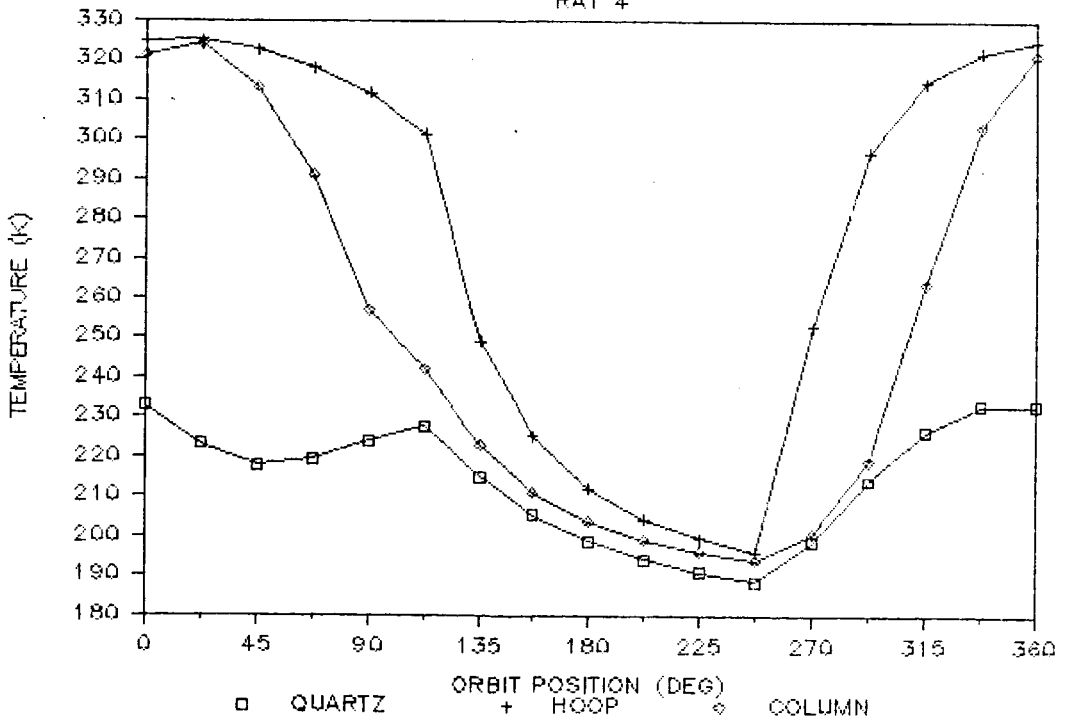
ELEMENT TEMPERATURE VARIATION FLIGHT

RAY 4



ELEMENT TEMPERATURE VARIATION FLIGHT

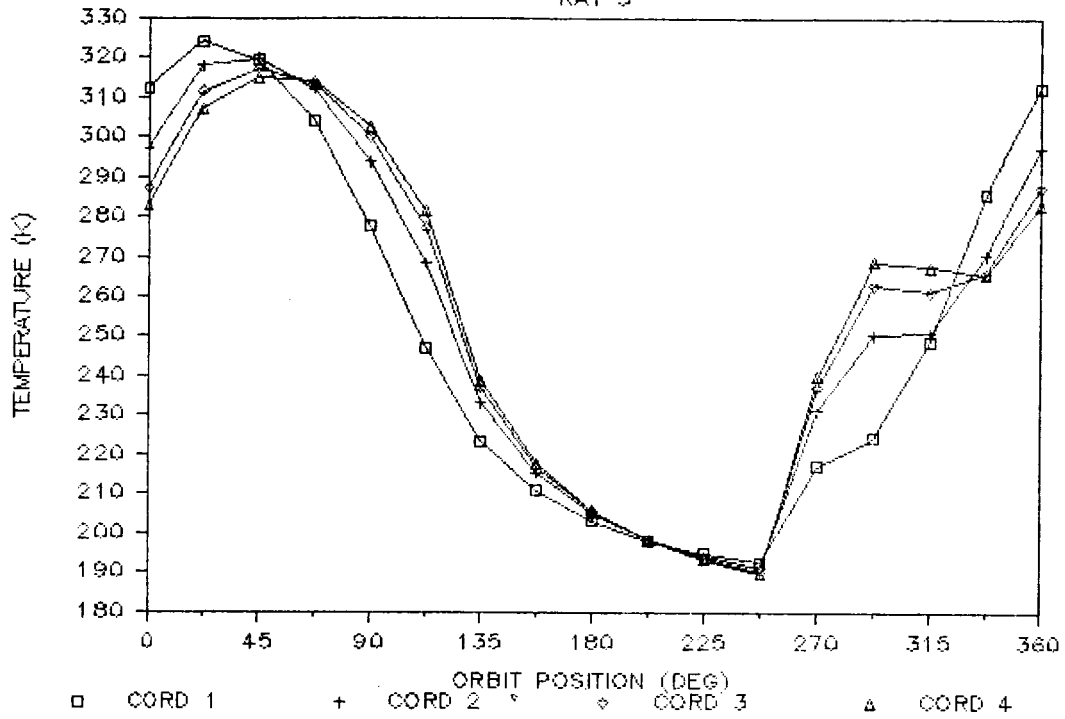
RAY 4



APPENDIX. ELEMENT TEMPERATURE VARIATIONS (CONT.)

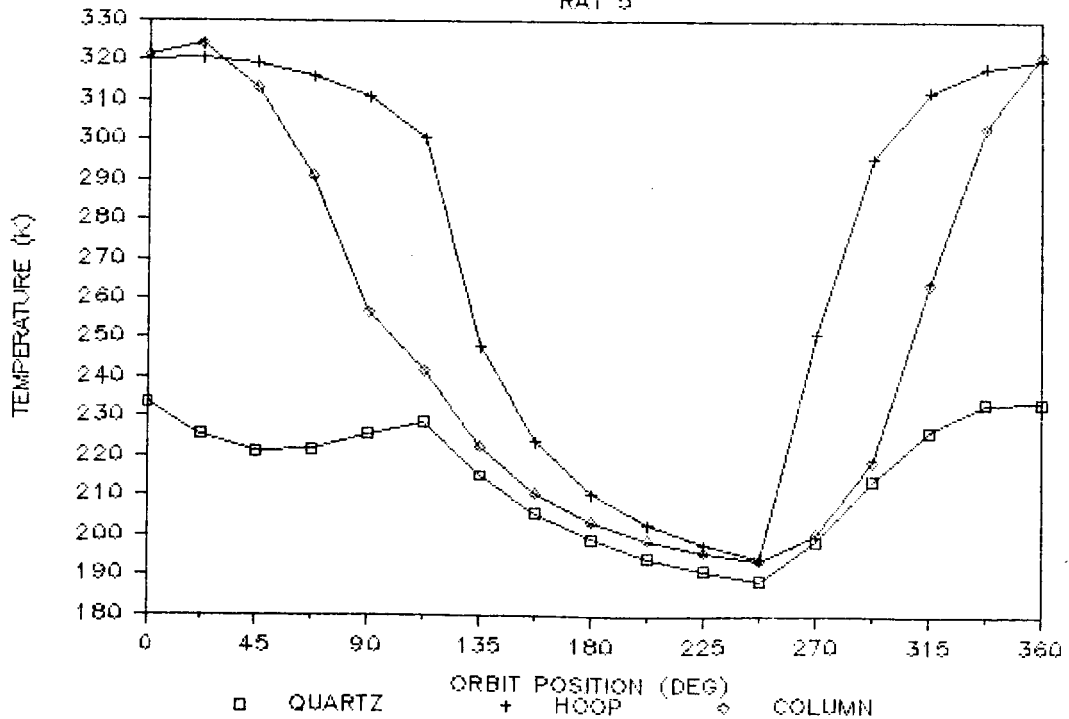
ELEMENT TEMPERATURE VARIATION FLIGHT

RAY 5



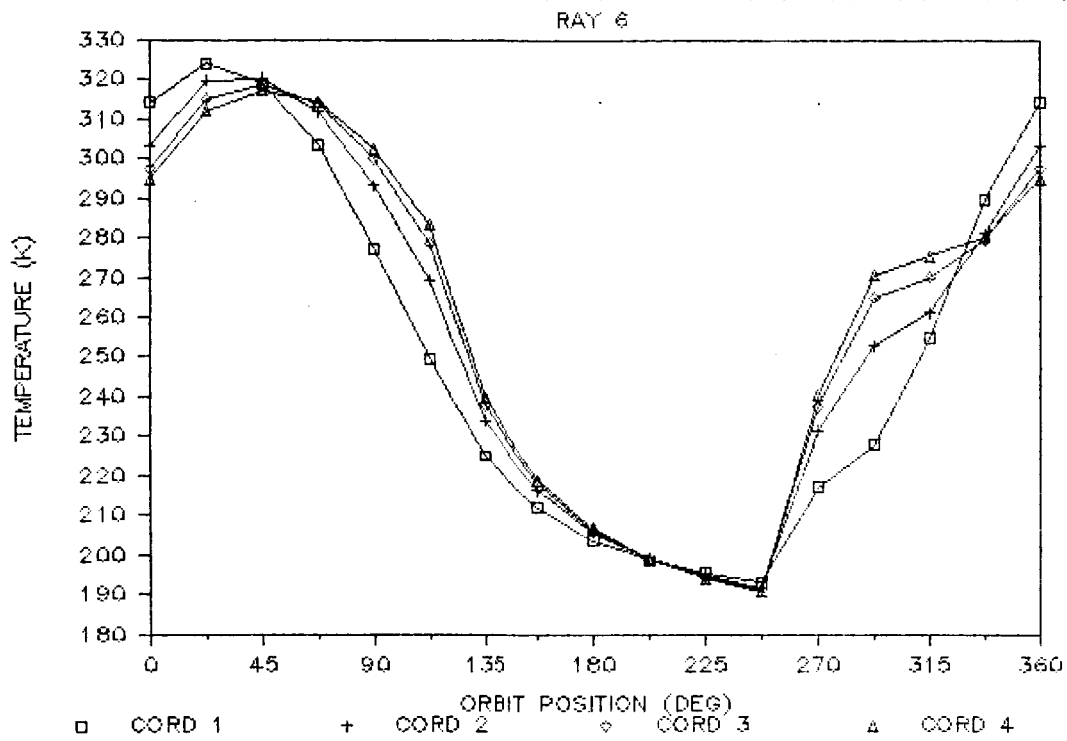
ELEMENT TEMPERATURE VARIATION FLIGHT

RAY 5

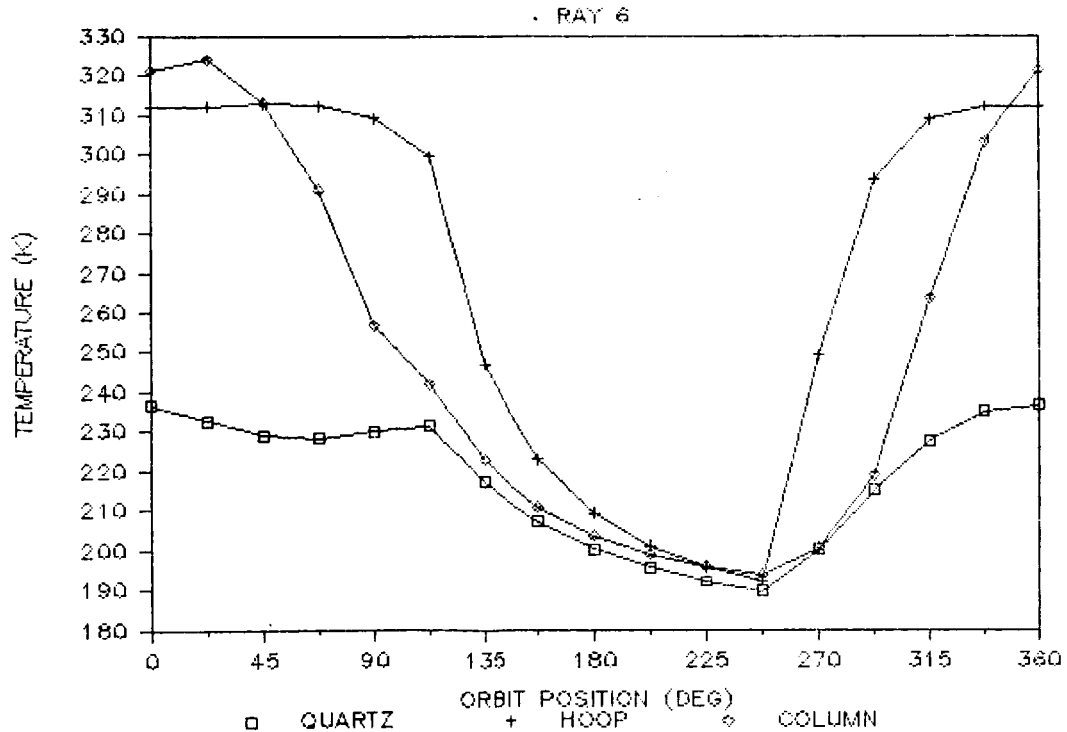


APPENDIX. ELEMENT TEMPERATURE VARIATIONS (CONT.)

ELEMENT TEMPERATURE VARIATION FLIGHT

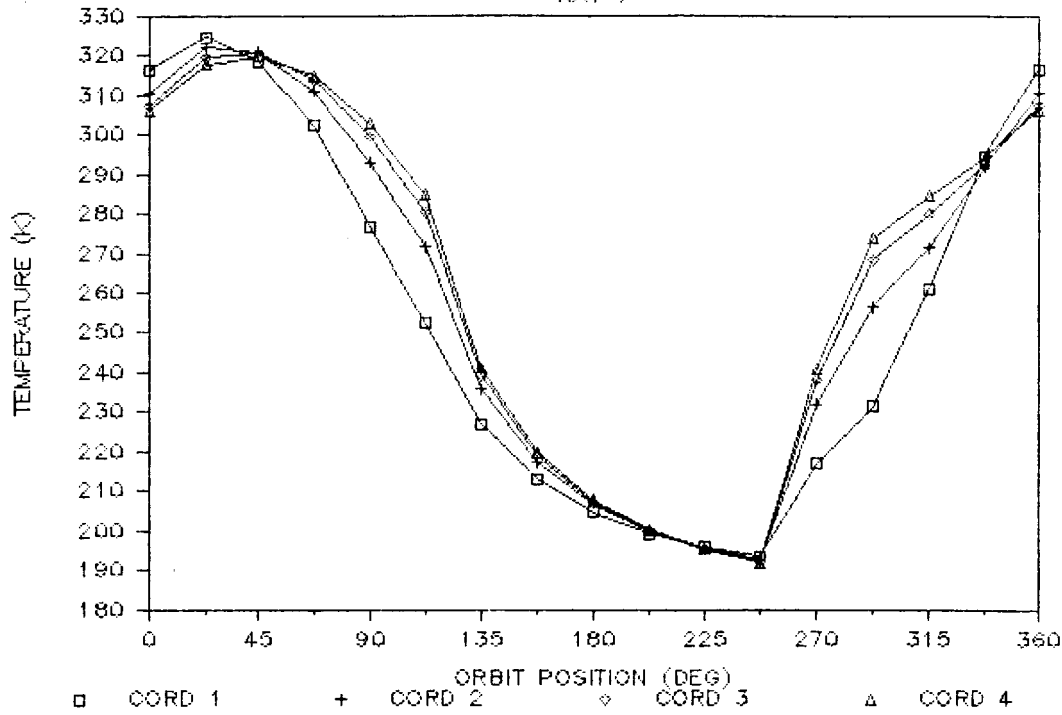


ELEMENT TEMPERATURE VARIATION FLIGHT

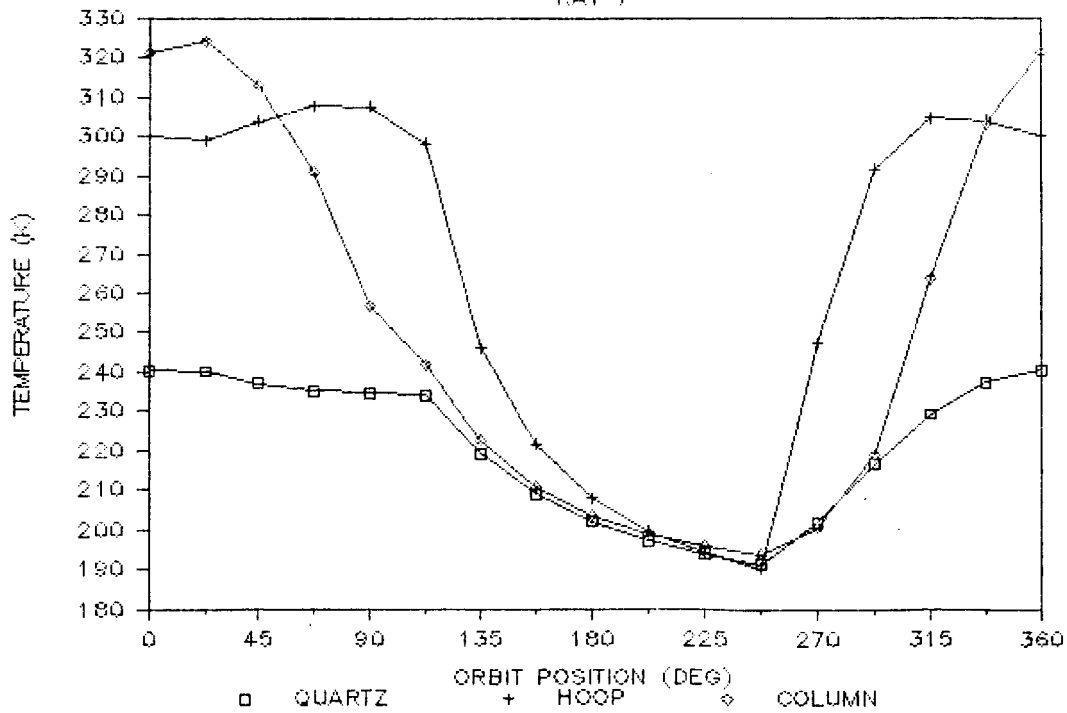


APPENDIX. ELEMENT TEMPERATURE VARIATIONS (CONT.)

ELEMENT TEMPERATURE VARIATION FLIGHT RAY 7



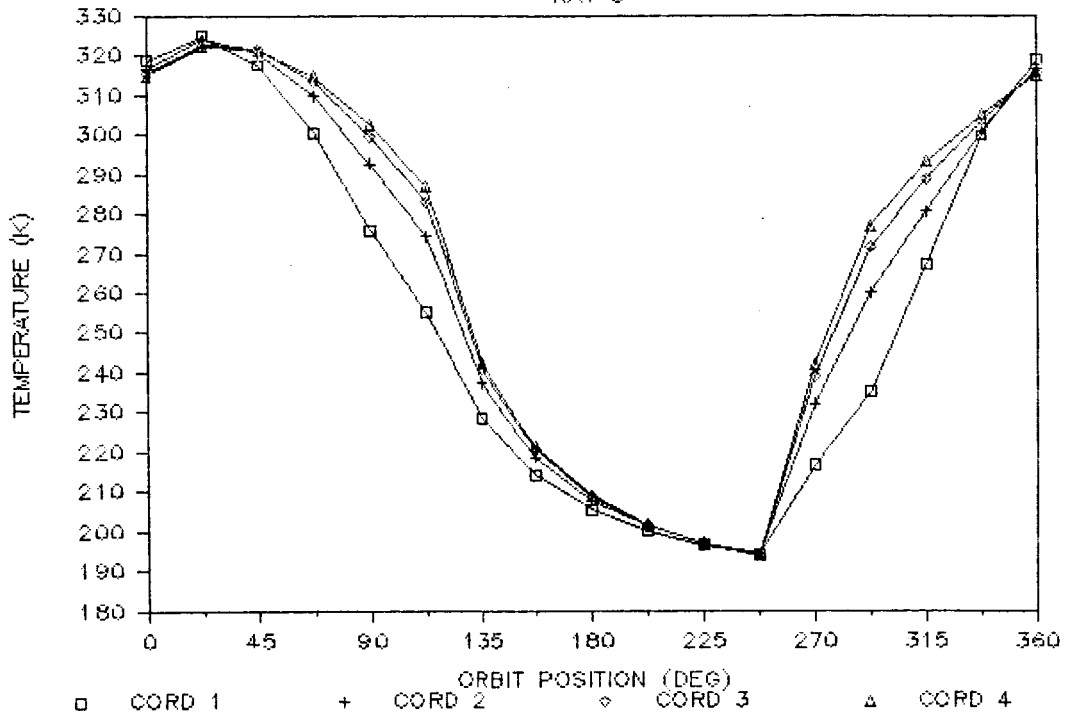
ELEMENT TEMPERATURE VARIATION FLIGHT RAY 7



APPENDIX. ELEMENT TEMPERATURE VARIATIONS (CONT.)

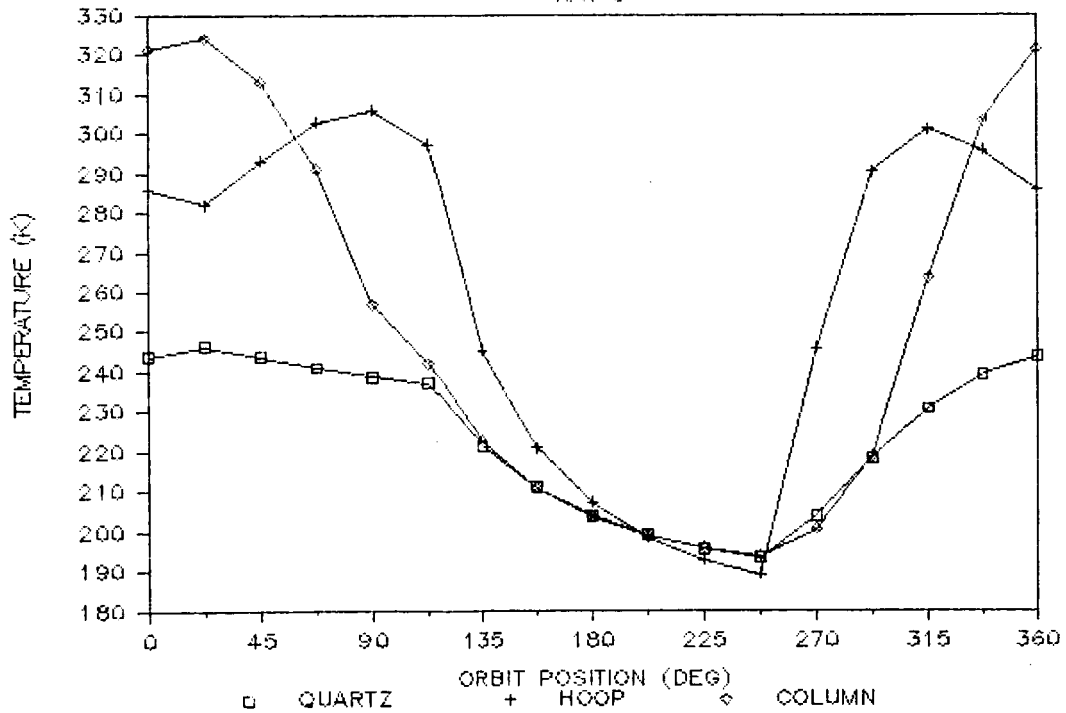
ELEMENT TEMPERATURE VARIATION FLIGHT

RAY 8



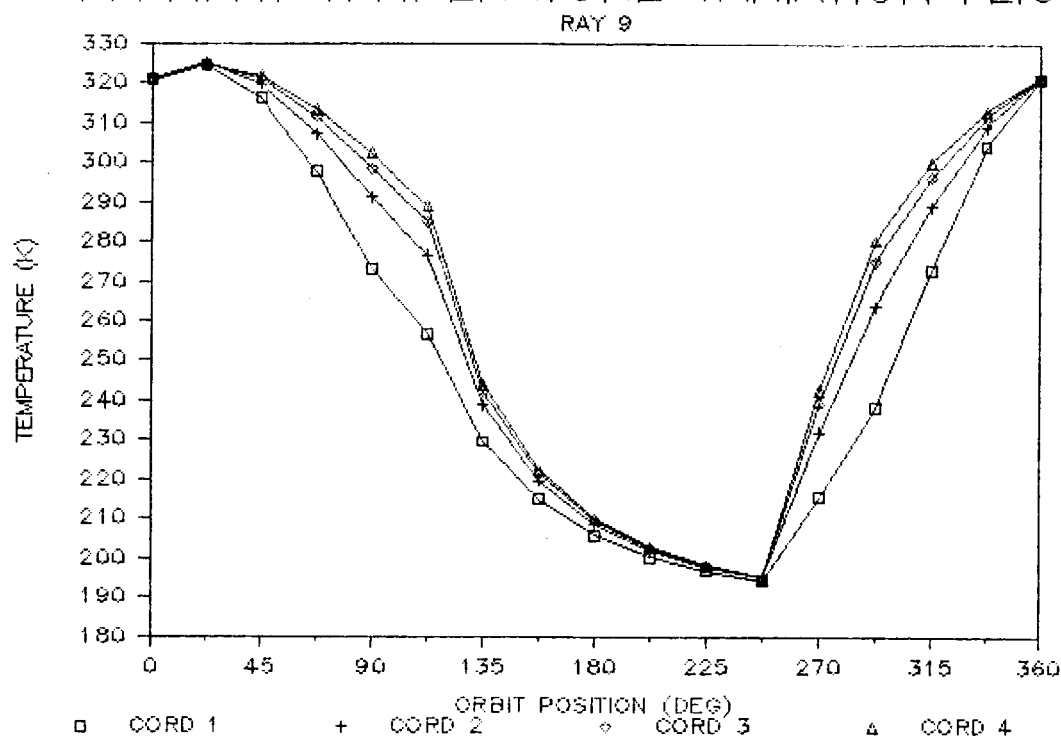
ELEMENT TEMPERATURE VARIATION FLIGHT

RAY 8

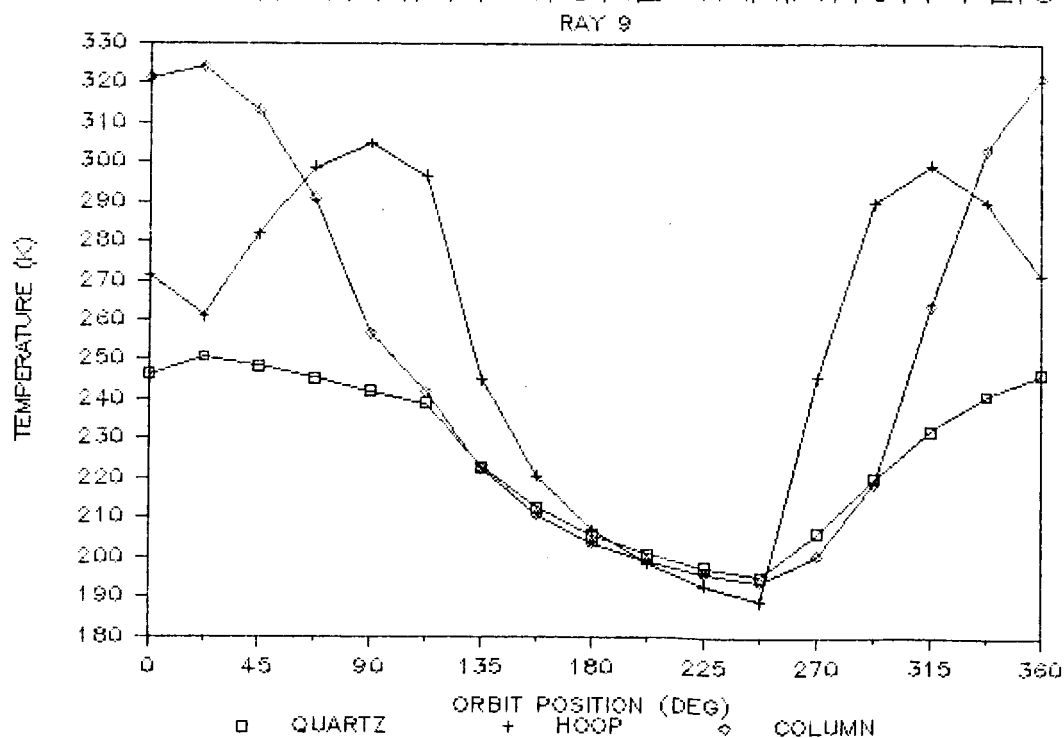


APPENDIX. ELEMENT TEMPERATURE VARIATIONS (CONT.)

ELEMENT TEMPERATURE VARIATION FLIGHT

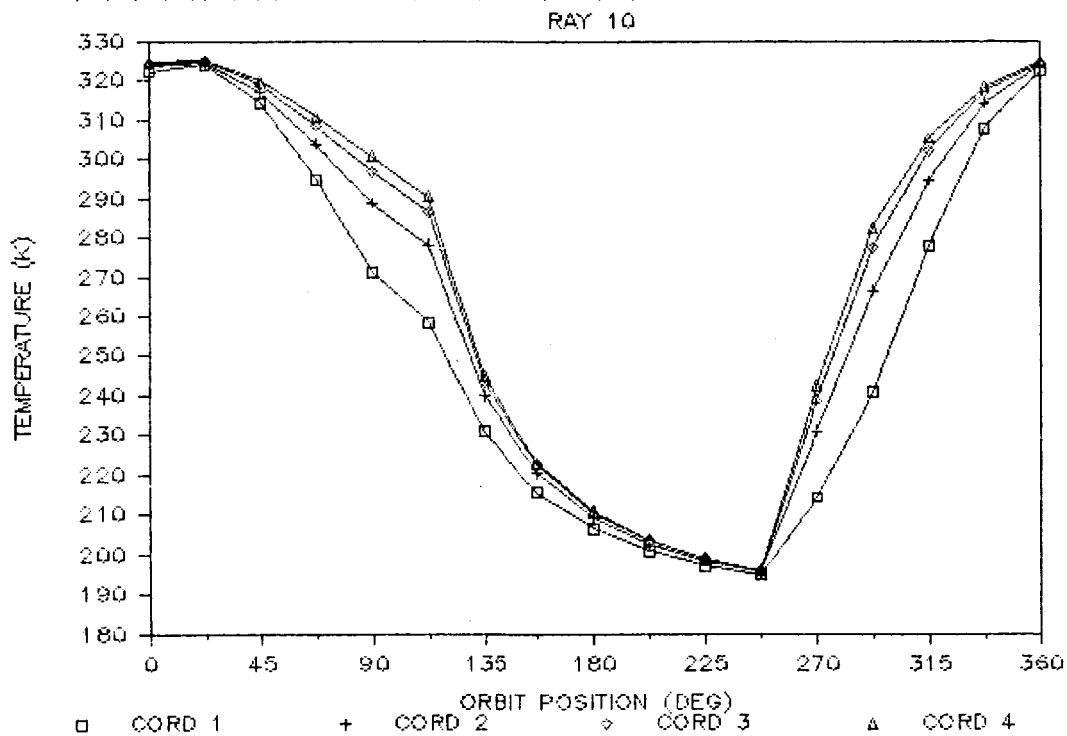


ELEMENT TEMPERATURE VARIATION FLIGHT

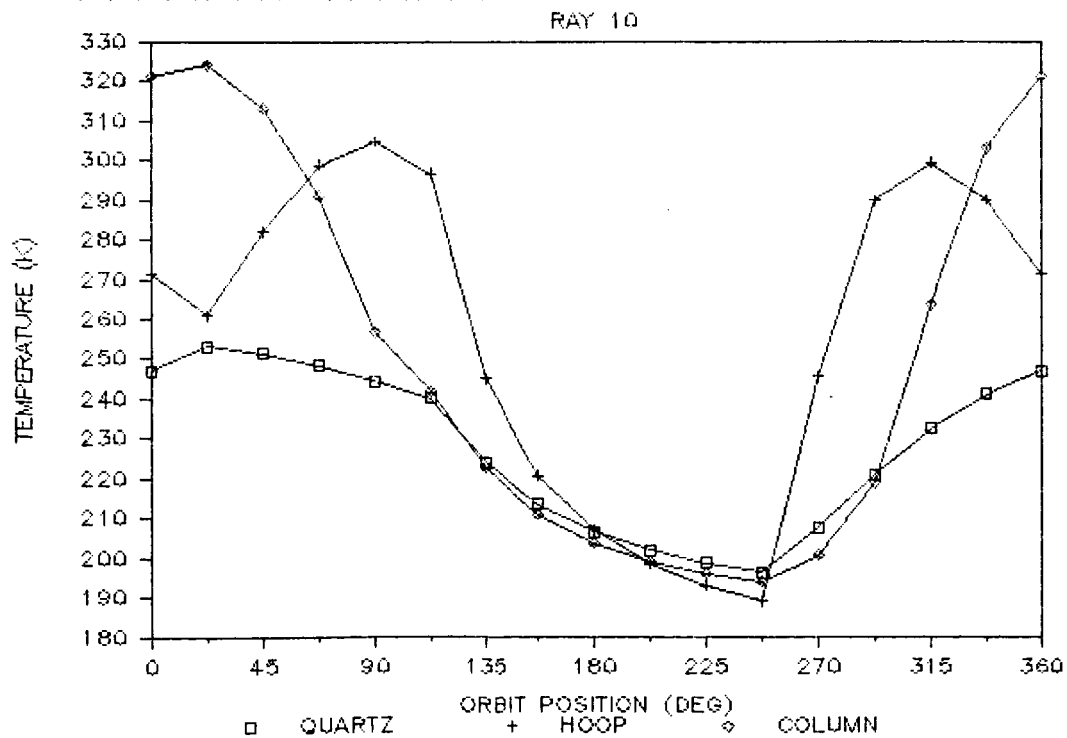


APPENDIX. ELEMENT TEMPERATURE VARIATIONS (CONT.)

ELEMENT TEMPERATURE VARIATION FLIGHT

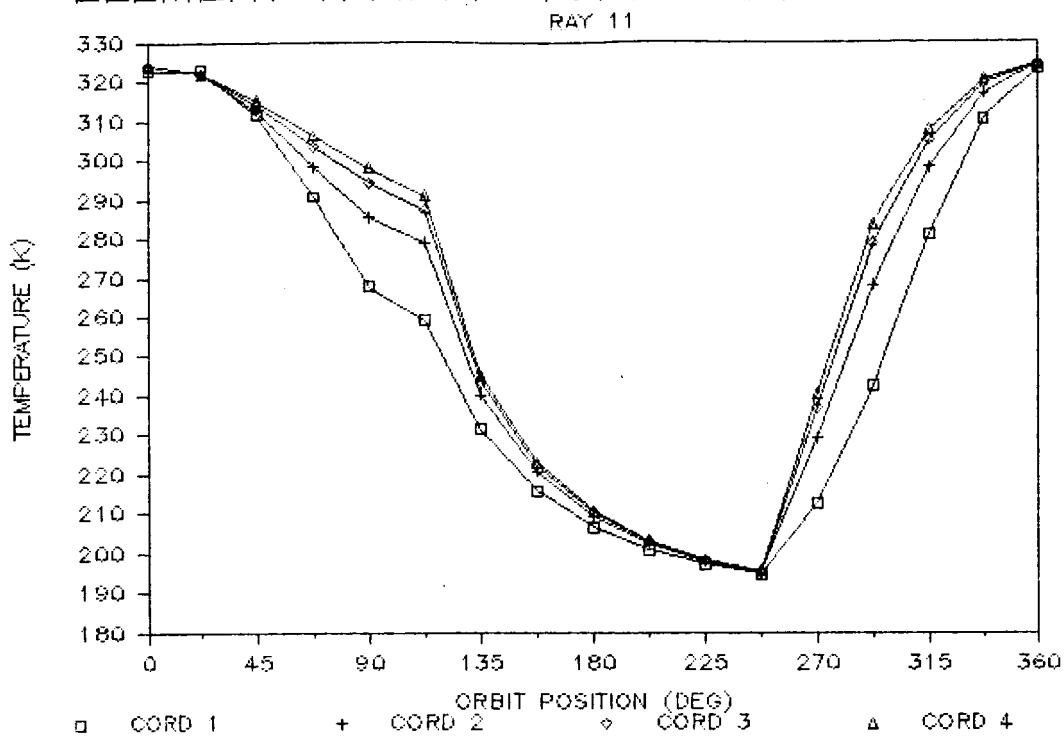


ELEMENT TEMPERATURE VARIATION FLIGHT

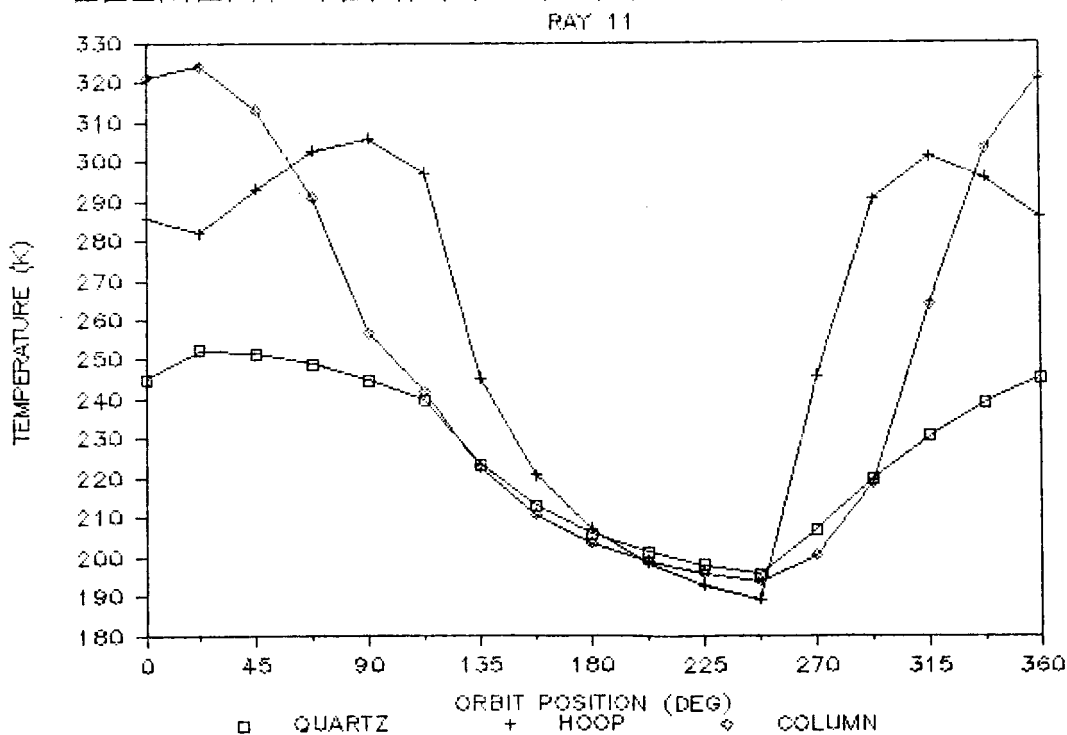


APPENDIX. ELEMENT TEMPERATURE VARIATIONS (CONT.)

ELEMENT TEMPERATURE VARIATION FLIGHT



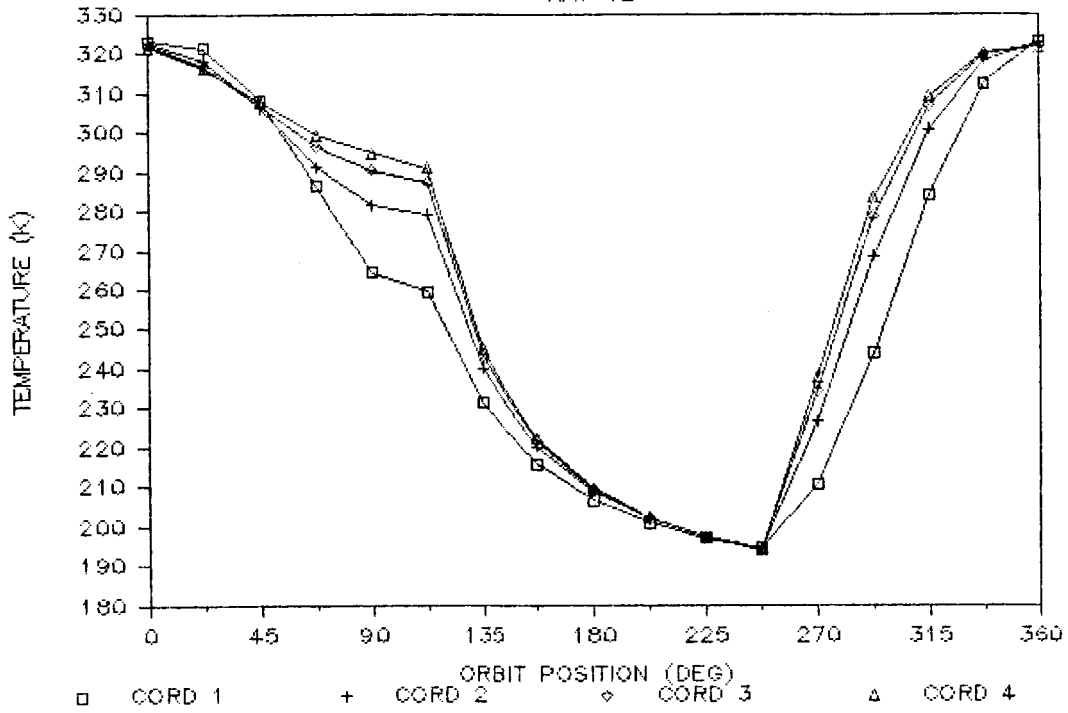
ELEMENT TEMPERATURE VARIATION FLIGHT



APPENDIX. ELEMENT TEMPERATURE VARIATIONS (CONT.)

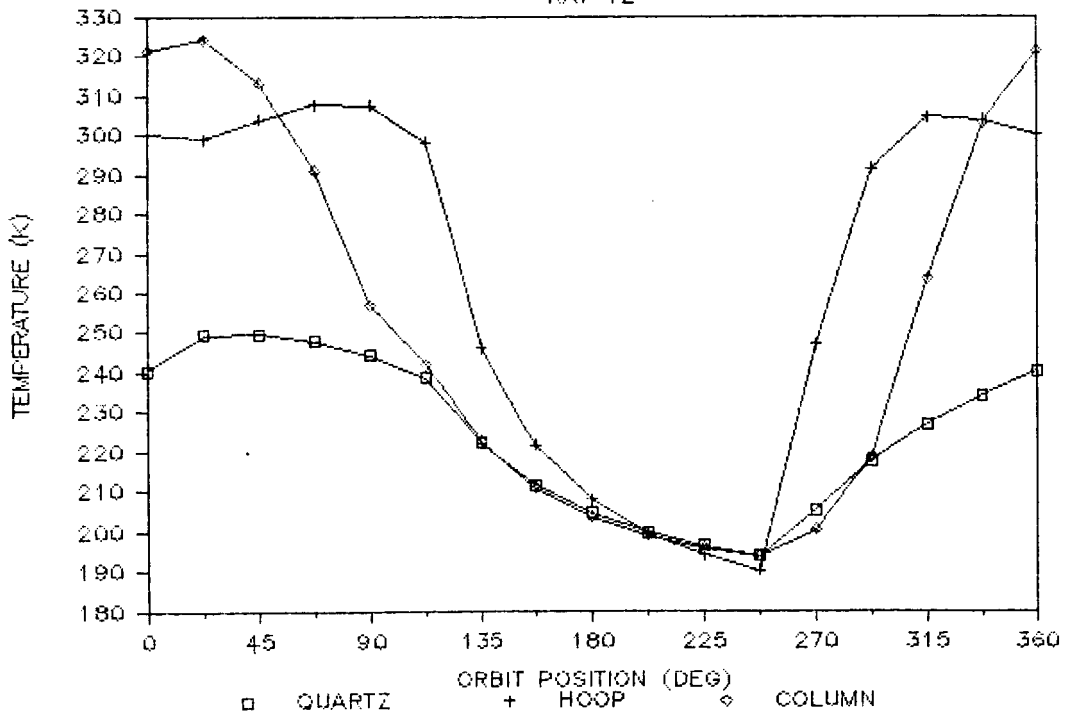
ELEMENT TEMPERATURE VARIATION FLIGHT

RAY 12



ELEMENT TEMPERATURE VARIATION FLIGHT

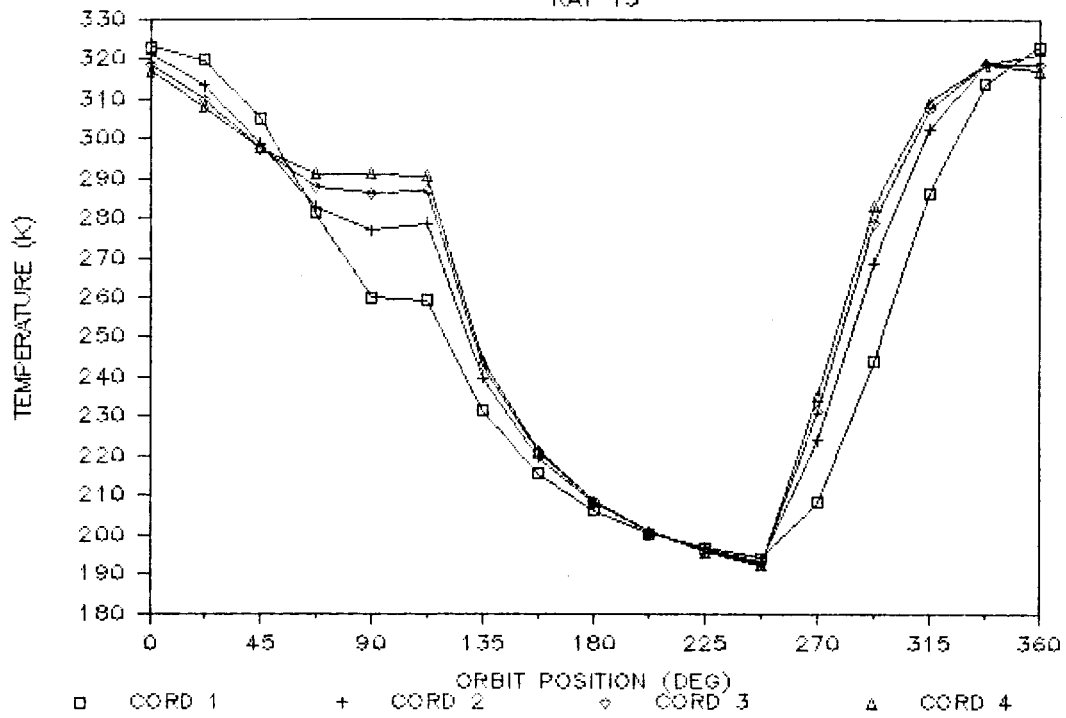
RAY 12



APPENDIX. ELEMENT TEMPERATURE VARIATIONS (CONT.)

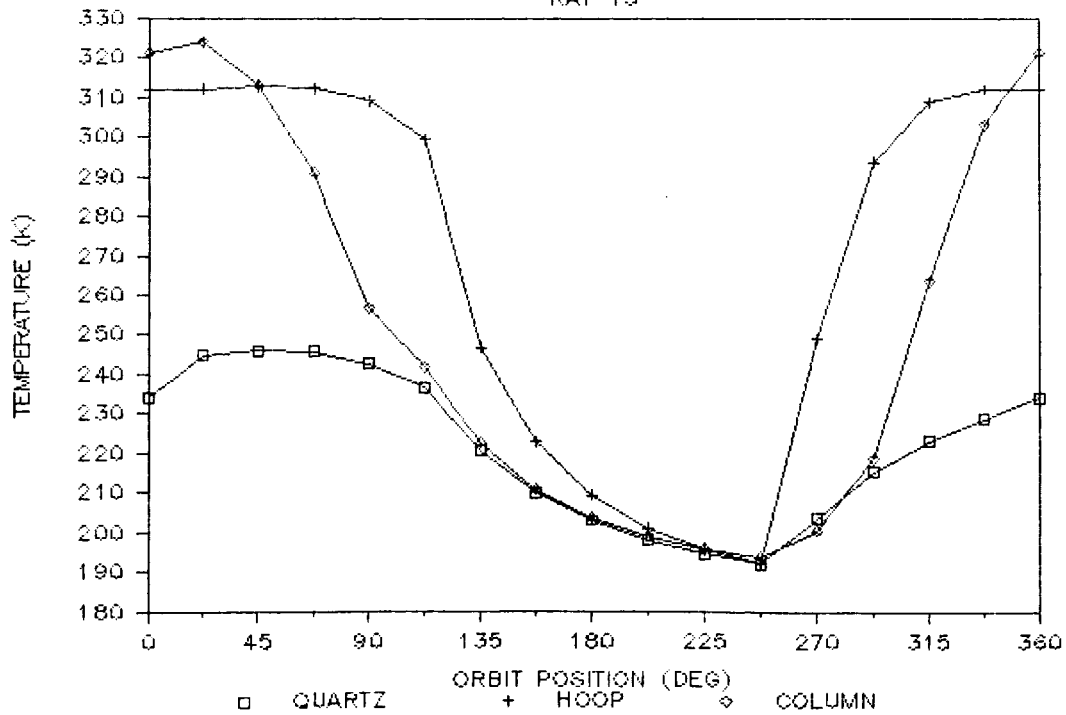
ELEMENT TEMPERATURE VARIATION FLIGHT

RAY 13



ELEMENT TEMPERATURE VARIATION FLIGHT

RAY 13



1. Report No. NASA TM-89137		2. Government Accession No.		3. Recipient's Catalog No.	
4. Title and Subtitle Analysis of On-Orbit Thermal Characteristics of the 15-Meter Hoop/Column Antenna				5. Report Date March 1987	
				6. Performing Organization Code	
7. Author(s) Gregory C. Andersen Jeffery T. Farmer James Garrison				8. Performing Organization Report No.	
				10. Work Unit No. 506-49-21	
9. Performing Organization Name and Address NASA Langley Research Center Hampton, Virginia 23665				11. Contract or Grant No.	
				13. Type of Report and Period Covered Technical Memorandum	
12. Sponsoring Agency Name and Address National Aeronautics and Space Administration Washington, DC 20546				14. Sponsoring Agency Code	
				15. Supplementary Notes Gregory C. Andersen and Jeffery T. Farmer, Langley Research Center, Hampton, VA James Garrison, Rensselaer Polytechnic Institute, Troy, New York	
16. Abstract <p>In recent years, interest in large deployable space antennae has led to the development of the 15-meter hoop/column antenna. This scaled down version of a proposed operational antenna concept can be used for both ground and on-orbit testing. This paper examines the thermal environment the antenna is expected to experience during orbit and determines the temperature distributions leading to reflector surface distortion errors. Two flight orientations corresponding to 1) normal operation and 2) use in a Shuttle-attached flight experiment are examined. A reduced element model was used to determine element temperatures at 16 orbit points for both flight orientations. The temperatures ranged from a minimum of 188 K to a maximum of 326 K. Based on the element temperatures, orbit positions leading to possible worst case surface distortions were determined, and the subsequent temperatures were used in a static finite-element analysis to quantify surface control cord deflections. The predicted changes in the control cord lengths were in the sub-millimeter ranges; however, the sensitivity of the reflective surface to control cord length changes can result in large surface distortion errors.</p>					
17. Key Words (Suggested by Author(s)) hoop/column thermal characteristics antenna			18. Distribution Statement Unclassified - Unlimited Subject Category 18		
19. Security Classif. (of this report) Unclassified		20. Security Classif. (of this page) Unclassified		21. No. of Pages 31	22. Price A03